NASA CR-134783
BCAC D6-42352

TITANIUM HONEYCOMB ACOUSTIC LINING
STRUCTURAL AND THERMAL TEST REPORT

(NASA-CR-134783) TITANIUM HONEYCOMB ACOUSTIC LINING STRUCTURAL AND THERMAL TEST REPORT Technical Report, Jan. - Aug. 1974 (Boeing Commercial Airplane Co., Seattle) 77 p HC $4.75 CSCL 20A G3/07

N75-21279

Unclas 18607

by D. Joynes and J. P. Balut

BOEING COMMERCIAL AIRPLANE COMPANY
A DIVISION OF
THE BOEING COMPANY

Prepared for

NATIONAL AERONAUTICS AND SPACE ADMINISTRATION

NASA Lewis Research Center

Contract NAS3-17842

1. Report No. NASA CR-134783	2. Government Accession No.	3. Recipient's Catalog No.
4. Title and Subtitle Titanium Honeycomb Acoustic Lining, Structural and Thermal Test Report		5. Report Date December 1974
		6. Performing Organization Code
7. Author(s) Donald Joynes and Jan P. Balut		8. Performing Organization Report No. D6-42352
		10. Work Unit No.
9. Performing Organization Name and Address Boeing Commercial Airplane Company P.O. Box 3707 Seattle, Washington 98124		11. Contract or Grant No. NAS3-17842
		13. Type of Report and Period Covered
12. Sponsoring Agency Name and Address National Aeronautics and Space Administration Washington, D.C. 20546		14. Sponsoring Agency Code Contractor Report

15. Supplementary Notes

Refan Project Manager, R. W. Schroeder
NASA Lewis Research Center, Cleveland, Ohio 44135

16. Abstract

This report presents the results of static, fatigue and thermal testing of titanium honeycomb acoustic panels representing the acoustic tailpipe for the Pratt and Whitney Aircraft JT8D Refan engine which is being studied for use on the Boeing 727-200 airplane.

Test specimens represented the engine and tailpipe flange joints, the rail to which the thrust reverser is attached and shear specimens of the tailpipe honeycomb. Specimens were made in four different batches with variations in configuration, materials and processes in each.

Static strength of all test specimens exceeded the design ultimate load requirements.

Fatigue test results confirmed that aluminum brazed titanium, as used in the Refan tailpipe design, meets the fatigue durability objectives.

Quality of welding was found to be critical to life, with substandard welding failing prematurely, whereas welding within the process specification exceeded the panel skin life.

Initial fatigue testing used short grip length bolts which failed prematurely. These were replaced with longer bolts and subsequent testing demonstrated the required life.

Thermal tests indicate that perforated skin acoustic honeycomb has approximately twice the heat transfer of solid skin honeycomb.

17. Key Words (Suggested by Author(s)) Boeing 727-200; Refan Engine Tailpipe; Acoustic Titanium Honeycomb; Aluminum Brazed Titanium; Fatigue Durability; Static Strength	18. Distribution Statement Unclassified - Unlimited

19. Security Classif. (of this report)	20. Security Classif. (of this page)	21. No. of Pages	22. Price*
Unclassified	Unclassified	80	

* For sale by the National Technical Information Service, Springfield, Virginia 22151

FOREWORD

The static, fatigue and thermal tests of the JT8D Refan acoustic tailpipe structural details described in this document were performed by the Structures Staff of the Boeing Commercial Airplane Company, a Division of the Boeing Company, Seattle, Washington. The work, sponsored by NASA Lewis Research Center and reported herein was performed between January and August 1974.

This report has been reviewed and is approved by

K. H. Hummel, Unit Chief
707/727/737 Structures Staff

4-8-75
Date

J. A. Ferrell, Chief Technology
JT8D Refan Program

4/10/75
Date

K. P. Rice
JT8D Refan Program

4/9/75
Date

TABLE OF CONTENTS

PRECEDING PAGE BLANK NOT FILMED

1.0 SUMMARY

This report presents the results of tests performed on titanium honeycomb acoustic panels used in the 727/JT8D NASA Refan program exhaust nozzle.

The purpose of the testing was to determine the static strength and fatigue durability of selected structural details, the heat transfer characteristics of titanium acoustic honeycomb panels, and to establish detail design features necessary to provide adequate strength and fatigue durability.

Three basic types of panels were structurally tested:

(a) Flange panels representing the engine aft flange and tailpipe joints.

(b) Rail panels representing the tailpipe rail members to which the thrust reverser is attached.

(c) Shear specimens representing the open edged honeycomb typical of the flange joints.

All three types of test specimens exceeded the ultimate static strength requirements and provided the design parameters so that the fatigue durability goals could be achieved.

During the flange panel fatigue tests, premature failures occurred in the flange attachment bolts. It was felt that longer bolts were required to meet the fatigue life objectives, and this was confirmed in subsequent testing using longer bolts with stacked washers under the head and nut.

Stress concentrations due to inadequate detail design and sub-standard welding were detrimental to fatigue life and precipitated premature failures. The fatigue durability obtained from acceptable quality welding exceeded the life requirements with failures occurring away from the weld zone in parent material.

Thermal tests were performed with flat, perforated and solid face sheet titanium honeycomb panels, subjected to engine exhaust gas efflux impingement typical of the tailpipe and thrust reverser door environment.

The heat transfer coefficient of the perforated acoustic honeycomb panel was determined to be approximately double that of the solid skin honeycomb.

2.0 INTRODUCTION

The NASA sponsored noise reduction and fuel economy investigation consisted of design and fabrication of hardware to retrofit the modified Pratt and Whitney Aircraft JT8D Refan engine in the Boeing 727-200 commercial airplane fleet.

In order to optimize engine noise attenuation with minimum weight increase, advanced structural concepts developed for the Boeing Supersonic Transport were utilized. For the engine tailpipe assembly, aluminum brazed titanium acoustic honeycomb was used. Comparative data for this and other titanium systems are shown in Reference 1a.

This report presents the results of static, fatigue and thermal tests which were conducted to provide design data for the acoustic tailpipe assembly.

The critical structural details were identified and test specimens representing them were manufactured in four different batches identified as A, B, C and D. Variations in specimen configuration, material and processing were allowed between each batch. Further test data were obtained from the Boeing SST follow-on program and was identified as batch A. See Reference 1b.

Specimens were subjected to structural static and fatigue testing using standard laboratory test machines, and to thermal testing using engine ground test equipment.

3.0 NOMENCLATURE

A	Area, sq. in.
BCAC	Boeing Commercial Airplane Company
b	Dimension, inches
d	Diameter, inches
e	Hole edge margin, inches
$f_{a_{max}}$	Fatigue alternating stress, maximum, lb per sq in
$f_{a_{min}}$	Fatigue alternating stress, minimum, lb per sq in
f_s	Applied shear stress, lb per sq in
f_t	Applied tensile stress, lb per sq in
F_{tu}	Material ultimate tensile stress, lb per sq in
GAG	Ground-air-ground. Once per flight fatigue load cycle.
h	Core depth, inches.
H_I	Gas heat transfer convection coefficient, in. B.T.U/Hr. in^2
H_O	Gas heat transfer convection coefficient, out. B.T.U/Hr. in^2
K_1	Conductivity coefficient front sheet. B.T.U/Hr. °F ft.
K_3	Conductivity coefficient aft sheet. B.T.U/Hr. °F ft.
K_{eff}	Effective heat transfer coefficient of core, B.T.U/Hr. °F ft.
L	Length, inches
N	Number of fatigue load cycles
P	Applied load, lb.
q	Heat flux. B.T.U/Hr.

PRECEDING PAGE BLANK NOT FILMED

3.0 NOMENCLATURE Cont'd

R	Fatigue stress ratio. $\frac{f_{a_{min}}}{f_{a_{max}}}$
t_f	Thickness, flange. inches
t_p	Thickness, perforated skin. inches
t_r	Thickness, rail. inches
t_s	Thickness, solid skin. inches
T_I	Gas Temperature, In. °F
T_o	Gas Temperature, Out. °F
ΔT	Temperature, °F
W	Width, inches

4.0 OBJECTIVES

These objectives cover the structural testing of both static and fatigue specimens as well as the determination of the heat transfer coefficients of titanium honeycomb structure.

4.1 STRUCTURAL TEST

The purpose of these tests was to obtain data that would ensure that the structural details for the tailpipe assembly could be designed to meet static strength and fatigue life requirements of the Refan installation. Variations in design, manufacturing process, and structural defects in the specimens were also evaluated.

The static strength requirements were that the test specimens shall be able to withstand loads representative of the refan tailpipe design ultimate loads.

The fatigue life criteria for the Refan installation was 20 years service life with 95% reliability and 95% confidence, which when based on a Weibull distribution, required a demonstrated test life of 100,000 cycles of ground-air-ground loading.

Static and fatigue load requirements were determined from the tailpipe structural analysis which is reported in the Phase II Refan Program Final Report.

4.2 THERMAL TEST

The purpose of this test was to determine the steady state heat transfer coefficient between face sheets of titanium honeycomb panels with either solid or perforated face sheet when exposed to engine exhaust gas efflux at impingement angles simulating the tailpipe and thrust reverser door.

5.0 TEST DESCRIPTION

The static, fatigue, and thermal tests applied to each panel are discussed in this section.

5.1 STRUCTURAL TEST

The testing was conducted in laboratory conditions at room temperature using standard test equipment. For the static tests, Baldwin Universal Test Machines of 120,000 lb. and 300,000 lb. capacity together with an Automatic Recorder were used. For the fatigue test a Sonntag Model SF-10-U, machine with a range of 5000 lb. mean load and ±5000 lb. alternating load was used.

Deflections and gaps were measured using dial and blade feeler gages. Strain gages were used on isolated specimens to confirm the accuracy of the methods of panel alignment. A special load fixture was developed for the rail panel test to apply simultaneously both radial and circumferential load to the panel and tension to the rail flange.

5.1.1 TEST SPECIMENS, GENERAL

Test specimens were made in four batches A, B, C, and D with variations in materials, dimensions and manufacturing methods between each batch.

Material was titanium 3 AL -2.5V for the core, and 6AL -4V for skins, flanges and rails with the exception of batches A and C which used CP 70 for the perforated skin. Test specimen materials and specifications are summarized in table 1.

Batch A and B panels used 4-25 core (4/16 inch square cell size and .0025 inch foil thickness), batch C used 6-20 core and batch D used 6-35 core which is specified for the Refan tailpipe.

PRECEDING PAGE BLANK NOT FILMED

Batches A, C, and D utilized aluminum brazing for core to face sheet attachment. Flanges and rails were welded to the face sheets using standard BCAC titanium welding procedures, batches A and C electron beam, and batch D used machine plasma arc. Some parts with substandard welding, weld repairs, and misalignment, were also included to obtain comparative test data.

In the batch B specimens, flange, rail, and core-to-skin faying surfaces were diffusion bonded using a proprietary process. All welds and faying surface bonds were made in .02 - .025 inch thick skin pads which were chemically milled down to .013 inch at approximately .25 inch away from the weld or joint line.

In order to simplify manufacture, the honeycomb panels were made as large flat units which were cut and reworked into the test specimens. It should be noted that since the test panels were flat, the tooling method used for the test panels was different from that used for the tailpipe hardware. The panels were subjected to BCAC standard quality control inspection procedures, i.e., ultrasonic and eddy current, to check core-to-face sheet braze, and radiography for the welds.

Manufacturing process and quality control specifications used for the test specimens batches A, C and D are documented in the SST Technology Follow-On Report -- Reference 1c.

5.1.2 FLANGE PANEL TEST

5.1.2.1 FLANGE PANEL TEST SPECIMENS

The flange panels represented the joints between the tailpipe sections and the engine case as illustrated in figure 1. The tailpipe flange panels were 7.0 inches wide with 2.0 inch bolt spacing and the engine to tailpipe joint panels were 9.0 inches wide with 3.0 inch bolt spacing. All flanges had three-bolt attachment to the loading fixtures.

The batch B and D panels had closed flange edge members, and the batch A and C panels had open edges similar to the tailpipe hardware as shown in figures 2 and 3.

Since the specimens were flat, the test loading fixtures and geometry of the test specimens were designed to obtain deflections similar to those of the cylindrical tailpipe when loaded.

For the batch A tests 1 and 2, two panels, 21.5 inches long, were loaded end to end in the test machine. This method presented deflection problems even though test 2 had the panels supported in the center to control out of plane deflection. Consequently, subsequent fatigue testing was done on single panels, and in order to obtain deflections compatible with the tailpipe, the panel length was reduced to 12 inches.

Batch A, tests 1, 2 and 3 are fully reported in Reference 1b.

Dimensions of the flange panels are given in table 2, and an illustration of the test set up is shown in figure 4.

5.1.2.2 FLANGE PANEL STATIC TEST

5.1.2.2.1 STATIC TEST LOADS

The flange panels were loaded by the test fixture flange through the three tension attachment bolts in a manner similar to the tailpipe hardware shown in figure 1.

From the structural analysis of the tailpipe,

Flange Bolt Maximum Load	= 2550 lb/bolt
With 2.0 Inch Bolt Spacing, Panel Load	= 1,275 lb/in of flange
Load on 7.0 Inch Panel	= 7 x 1275 = 8,925 lb.
Load on 9.0 Inch Panel	= 9 x 1275 = 11,475 lb.

5.1.2.2.2 FLANGE PANELS STATIC TEST RESULTS

All flange panels exceeded the ultimate design load requirements. Failure occurred in the chem-milled radius of the outer sheet in all cases. An exception occurred on one panel which failed the nut plate strap, which in turn precipitated failure of two bolts at the thread. This panel was subsequently retested with nuts compatible with bolt strength and failed in the chem-milled radius of the outer sheet.

The test results are summarized in table 3. Typical static failure is shown in figures 2 and 5 and the nut plate strap failure in figure 6.

5.1.2.3 FLANGE PANEL FATIGUE TEST

5.1.2.3.1 FATIGUE TEST LOADS

The flange panel loads represent the engine flange attachment fatigue spectrum loads reduced to a ground-air-ground (G.A.G.) cycle to simplify testing.

Flange G.A.G. Load Maximum	= 525 lb/in
Minimum	= 50 lb/in
Stress Ratio R	= 0.10
Load on 7.0 Inch Panel	= 7 x 525 = 3675 lb
Load on 9.0 Inch Panel	= 9 x 525 = 4725 lb

Where specimens were tested at other than the GAG load cycle, the equivalent number of cycles was obtained by using the BCAC fatigue relative life analysis.

5.1.2.3.2 FLANGE PANEL FATIGUE TEST RESULTS

Although the tests were primarily for the flange panels, a significant number of attachment bolt failures occurred. These failures are discussed below under Flange Panel Bolt Failures.

<u>Flange Panel Fatigue Test</u>

The double specimen setup and long panels used for the batch A test No. 2 resulted in unrealistic panel deflection and consequent early failure of the flange. For the 2nd test, with the panel supported at the center to control deflection, it exceeded the required life and failed in the chem-milled radius of the solid skin.

All three batch B specimens failed in the skin at the junction with the flange leg runout short of the required life. This joint had a high stress concentration factor due to the excessive flange-leg to skin-thickness ratio, and negligible fillet radii inherent with the liquid diffusion bond process. Faying surface bond was marginal due to local flange warping and may also have contributed to the low lives obtained.

Both batch C specimens tested fully exceeded the required life, with failures occurring in the flange radius and bolt holes. One specimen was damaged when the bolts failed and so fatigue testing had to be terminated prior to any fatigue damage to the panel or flanges.

One batch D specimen exceeded the life required and failed in the center of the outer skin. The other two failed prematurely at the skin-to-flange weld, which was substandard and had skin misalignment and distortion.

Results of panel tests are given in table 4 and typical failures are illustrated in figures 7, 8, and 9. The demonstrated fatigue curves for skin weld and flange,determined from the test results are plotted in figures 10 and 11. Refer to the appendix for summary of fatigue reduction method.

Flange Panel Bolt Failures

During the flange panel fatigue tests a number of failures occurred to both the 1/4 dia. and 5/16 dia. flange attachment bolts.

Failures were at random attachment locations with the bolts fracturing both in the shank and the thread runout.

Analysis of the flange joint test results indicated that flange bending introduced eccentric loading of the bolts, which were too stiff when compared to the flanges. To obtain compatible flange and bolt stiffness, longer bolts with stacked washers under the head and nut were substituted and subsequent testing was carried out without further failures. See Figure 12.

Bolt failures are tabulated in table 5 and the plotted demonstrated fatigue life in figure 13.

5.1.3 RAIL PANEL TEST

5.1.3.1 RAIL PANEL TEST SPECIMENS.

The rail panels represented the tailpipe rail, to which the thrust reverser support fitting is attached. A typical rail panel test setup is shown in figure 14 and dimensions of the specimens are given in table 6. The machined rails were electron beam welded to the solid skin for the batch C panels and machine plasma arc welded for batch D, which also had some hand weld repair areas. Batch B rails were diffusion bonded to a continuous solid skin. Skins and rails were either aluminum brazed or diffusion bonded to the core to become an integral part of the panel.

Refer to Table 6 for rail panel dimensions.

5.1.3.2 RAIL PANEL TEST LOADING

The panel was loaded simultaneously radially and transversely which consequently required a special loading fixture. The ratio of radial load to transverse load was determined from the tailpipe structural model and was fixed by the test fixture geometry as shown in figures 15 and 16.

The rail panel was cantilevered from the test fixture, with the free end supported by the adjustable diagonal struts which induced a transverse load and bending into the panel when a radial load was applied to the rail. This system duplicated the tailpipe circumferential loads and rail loading from the thrust reverser.

5.1.3.3 RAIL PANEL STATIC TESTS

5.1.3.3.1 RAIL PANEL STATIC LOADS

Rail panel static loads were determined from analysis of thrust reverser operation at maximum design placard speeds.

From structural analysis maximum load on rail = 3500 lb. ultimate. For 7.0 Inch Rail Maximum Load = 2,700 lb. ultimate. Transverse Tension Load in Rail Panel induced by Test Fixture Rail Load for:

9.0 In. Panel = 2 x 3,500 = 7,000 lb.
7.0 In. Panel = 2 x 2,700 = 5,400 lb.

For rail loading diagram, see figure 16.

5.1.3.3.2 RAIL PANEL STATIC TEST RESULTS

The batch B panel failed in the skin adjacent to the chem-milled radius. Initial shear failure of the lighter 6-20 core of the batch C panel allowed the panel to bow, which resulted in a skin and core tension failure at considerably higher load, as shown in figure 17. The batch D panel failed in the weld which was of marginal quality, see figure 18.

Static test results are shown in Table 7.

5.1.3.4 RAIL PANEL FATIGUE TEST

5.1.3.4.1 RAIL PANEL FATIGUE LOAD

The fatigue loads represents the loads from a normal operation reverse-thrust cycle.

G.A.G. Max. Load for 9.0 in. Rail = 1400 lb.
Stress Ratio R = 0.10.

5.1.3.4.2 RAIL PANEL FATIGUE TEST RESULTS

Two of the batch B panels exceeded the required life with failures occurring in the skin adjacent to the chem-milled radius. The third most highly loaded panel failed in core shear, buckling the perforated skin. Failures occurred at low cycles in all three batch C panels which failed in core shear allowing the panel to deform. Batch D panels failed in the welds at repair locations. Typical failures are shown in figures 19 and 20.

Batch B rail and flange panels had a similar detail at the runout to-skin junction, however, the rail-panel skin was continuous, and the associated improvement in stress concentration moved the fatigue critical detail to the chem-milled radius which resulted in considerable life improvement.

Core strength and thickness was critical for the rail panels due to the induced shear from bending and the rail tension load. The high rail load and associated core shear may have precipitated failure of the perforated skin and core at the relatively low life seen in test number 4. High bending stress and shear due to the thin, .375 in. panel and 6-20 core caused early core shear failures in the batch C panels, and resulted in panel deformation but no failures in the skins. Figure 19 illustrates a typical shear failure.

Fatigue test results are summarized in table 8 and demonstrated life plotted in curve figure 21.

5.1.4 SHEAR SPECIMEN TEST

5.1.4.1 SHEAR TEST SPECIMENS

The shear specimens simulated the core loading at the tailpipe flange joint, having both open core and load application to the outer skin.

The test specimens were cut from the large panels in pairs, each individual coupon being made by cutting the solid skin and core. Two pairs were mounted back to back in the test machine with the load applied through the solid skin so that four coupons were tested simultaneously. Some specimens had a .125 in. thick aluminum doubler bonded to the solid skin in order to support the skin at the test machine grips. See figures 22 and 23 for coupon details and typical installation.

5.1.4.2 SHEAR SPECIMEN STATIC TEST

5.1.4.2.1 SHEAR SPECIMEN STATIC LOADS

Shear specimen static loads were derived from the tailpipe design ultimate load conditions for the tailpipe flange taking into account deformation of the core.

Ultimate core shear load

= 210 lb/sq. in.

Test load requirement for 2.0 x 2.0 coupon mounted back to back

= 210 x 4 x 2 = 1680 lb.

5.1.4.2.2 SHEAR SPECIMEN STATIC TEST RESULTS

Both specimens tested exceeded the ultimate design load requirements. Local bending of the solid skin at the test machine grips induced tension stresses in the core and bond line which initiated a pealing type failure originating at the edge of the core.

The undamaged specimens from each test were salvaged and used as a pair in the fatigue test.

Test results are shown in table 10 and the static failures in figure 24.

5.1.4.3 SHEAR SPECIMEN FATIGUE TEST

5.1.4.3.1 SHEAR SPECIMEN FATIGUE LOADS

The fatigue loads are based on engine and thrust reverser normal operation and shear loads obtained by redistributing flange joint loads into the panel using elastic analysis of the core and skins.

Core Shear = 130 lb/sq. in.

For 2.0 x 2.0 Test Coupon mounted back to back

Test Load = 130 x 4.0 x 2 = 1040 lb.

5.1.4.3.2 SHEAR SPECIMEN FATIGUE TEST RESULTS

Low lives were obtained from the initial tests and as with the static test specimens, failures were attributed to local solid skin bending at the test machine clamps applying tension loads, unique to the mounting of the test specimen, which precipitated premature core failures. To obtain valid core shear data, the solid skin was reinforced by bonding to it a .125 in. aluminum doubler. Subsequent test specimens failed in core shear and the life objectives were achieved.

The batch C 6-20 core coupons failed in shear, at low lives consistent with the lower density core.

Test results are summarized in table 11 and typical failures shown in figure 25. The core shear fatigue curve is shown in figure 26.

5.2 THERMAL TEST

This test was conducted using an engine ground test rig with the test panels subjected to the engine exhaust gas efflux to simulate tailpipe and thrust reverser door service environment.

5.2.1 TEST DESCRIPTION

Two flat .50 in. thick honeycomb panels manufactured in batch B, panel number 1 with 10% perforated face sheet and panel number 2 with solid front face sheet and solid rear face sheet were tested in an impinging hot gas stream to determine the temperature gradient across the honeycomb. The panels were instrumented and mounted on a test box which was used to obtain a controlled atmosphere behind the panels.

A JT8D-1 prototype engine, which has a maximum engine exhaust gas temperature (EGT) of about 916°F, was mounted on a ground test rig with the test panel box set up in the exhaust gas efflux.

The test box was force ventilated to obtain a controlled environment on the rear face sheet of the test panels and could also be rotated to accommodate the exhaust gas impingement angles required in the test.

Tests were made with panels set at 6°, 75° and 90° impingement angles to the engine efflux and at power settings to simulate refused takeoff and normal reverse thrust cycle operations.

Instrumentation for each honeycomb panel consisted of 6 thermocouples attached to the back surface of the front and rear face sheets on the panel center line. In addition, one thermocouple was placed 1/2" in front of the test panel and a second thermocouple in the insulated box behind the panel to record gas and air temperatures respectively.

All data were recorded for stabilized conditions after 30 seconds at the test power setting.

Diagram of the test configuration is shown in figure 27.

5.2.2 THERMAL TEST RESULTS

All temperature data were recorded with the exception of the three thermocouples on the forward face sheet of the solid panel which were damaged during testing. The test data plotted in figures 28 and 29 are the average of these runs, and includes estimated values for the damaged thermocouples.

A heat transfer analysis, programmed for IBM 6600 computer, was used to determine the panel effective coefficient of conductivity, to match the estimated linear curves through the experimental data at a particular gas temperature, and to estimate the solid forward face sheet temperatures. The same program then used this effective coefficient of conductivity, together with the convection heat transfer coefficients needed to match the experimental data for the hot gas to the forward face sheet and the rear face sheet to the cooling box flow, to extrapolate the engine gas temperature to 1100°F and also to reduce the data to standard day, normal operational conditions.

Formulae used in this heat transfer analysis are shown in the Appendix.

These data are plotted in figures 30, 31, 32 and 33.

Initial analysis of the 6° impingement test indicated that it was not critical and due to budget limitations data reduction was not completed.

6.0 CONCLUSIONS

These tests successfully qualified the selected material processes and design concepts for use in the Refan tail pipe in both the static and fatigue environments.

6.1 STRUCTURAL TEST

6.1.1 STATIC TEST

All static test specimens exceeded the design requirements. However, minimum test values were associated with the quality of welds and test specimen preparation. Where welding quality was within the process specifications test results were high, with failures occurring in parent material. The shear coupon failures were due to combined skin peeling and shear and therefore do not represent true core shear values which would probably be higher than those recorded in the tests.

6.1.2 FATIGUE TEST

The fatigue test results demonstrated that the fatigue durability requirements of the Refan program tailpipe could be achieved.

The chem-milled skin, machined flanges and rails exceeded the design fatigue objectives, as also did the aluminum brazed titanium honeycomb and skin welding where both were to the final design specification and manufactured within the process specification tolerances.

Premature failures in the flange attachment bolts were resolved by the use of longer bolts to achieve the desired fatigue life. Both the bolt and flange failures indicate the flexibility of this joint and so stiffening the flanges would also have resulted in extending the bolt life.

Premature failures also occurred in the welds of both the flange and rail panels. These failures were due to improper weld processing, skin to flange runout misalignment, hand weld repair and underfill. However, weld life was in excess of the parent material where weld quality was within the process specifications. Batch B flange panels failed prematurely at the flange runout to skin junction due to the high stress concentration factor for this detail. Further design refinements would be required to eliminate this problem to achieve the design fatigue objective.

Batch B rail and flange panels had similar details at the runouts to skin junction, however, the rail panel skin was continuous, and the associated reduction in stress concentration moved the fatigue critical detail to the chem-milled radius which resulted in considerable life improvement.

Flange cracks originating in the attachment holes in the fillet radii were due to local flange bending, but were not considered significant since the panels had exceeded the life requirements as shown in figure 12. No problems were associated with either the open or closed edge honeycomb flange members.

As seen in the static test, shear specimens failed in tension at the edge of the core because the solid skin was not supported at the test machine grips. With the solid skin supported by the bonded doubler core shear failures occurred and core shear durability was demonstrated.

The light, 6-20 core used in the batch C panels did not meet the life requirements in either the rail or shear specimens and would not be acceptable for the tailpipe core.

Voids between the flanges, skins and core were evident in some specimens prior to testing, however no direct correlation was established between these areas and test failures.

To summarize, manufacturing the tailpipe by welding the machined flanges and rails to the outer skin, and using 0.013 in. solid skin and 0.014 in. perforated inner skin aluminum brazed to 6-35 titanium core meet the 727 JT8D Refan tailpipe fatigue durability requirements. High quality welding within the process specifications for both the flange and rail to skin attachment must be maintained to meet the fatigue durability requirements.

6.2 THERMAL TEST

No appreciable temperature differences were noted between either the simulated refused takeoff or normal reverser conditions, or as a result of the 75° or 90° gas impingement angle. Data scatter was about 35° after 30 seconds elapsed time as can be seen in figures 28 and 29.

The estimated perforated panel effective coefficient of thermal conductivity, K_{eff}, was .47 compared to an estimated K_{eff} of .21 for the solid face sheet panel. This results in a temperature differential through the panel of 280°F and 455°F respectively at EGT of 1100°F on a standard day.

7.0 FIGURES AND TABLES

FIGURES

TABLES

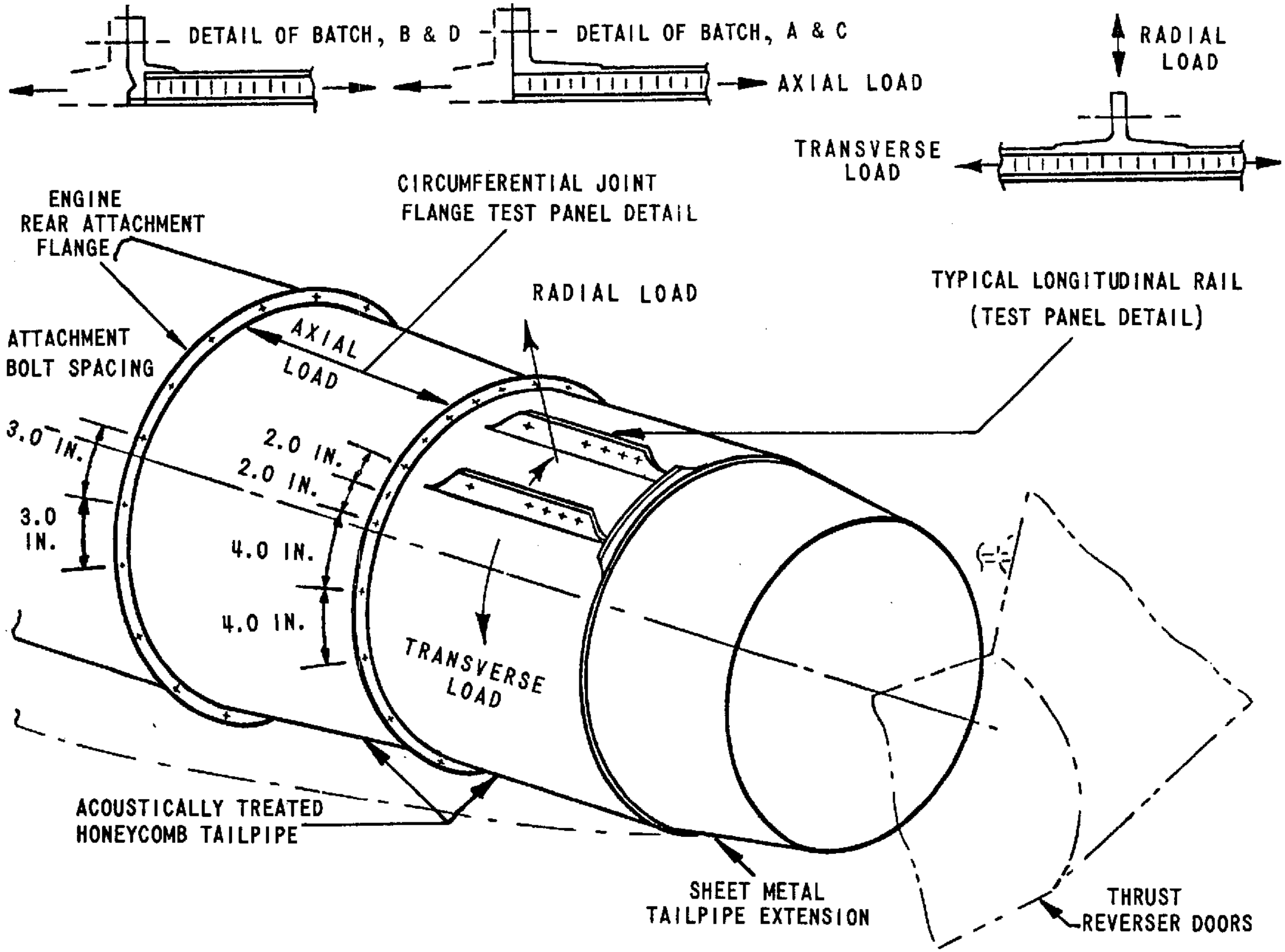

FIGURE 1. DIAGRAM OF TAILPIPE ASSEMBLY 727/JT8D REFAN

TABLE 1. TEST SPECIMEN MATERIAL

BATCH	SOLID SKIN	PERFORATED SKIN	CORE	FLANGE	RAIL.	FLANGE & RAIL ATTACH.	SKIN TO CORE ATTACH
A	6AL-4V	C.P.70	3AL-2½V	6AL-4V BAR		ELECTRON BEAM WELD	TI. AL. BRAZE
B	6AL-4V	6AL-4V	3AL-2½V	6AL-4V	6AL-4V	LIQUID DIFFUS'N BOND	LIQUID DIFFUS'N BOND
C	6AL-4V	C.P.70	3AL-2½V	6AL-4V BAR	6AL-4V EXTRUSION	ELECTRON BEAM WELD	TI. AL. BRAZE
D	6AL-4V	6AL-4V	3AL-2½V	6AL-4V BAR	6AL-4V BAR	MACHINE PLASMA ARC	TI. AL. BRAZE

SKIN SPEC.; MIL T 9046 F TYPE 3
CORE SPEC.; BOEING SPEC. XBMS 4 12 E
BAR SPEC. ; MIL T 9047
EXTRUSION SPEC.; MIL T 8156
FLANGE PANEL TEST ATTACHMENTS
BOLTS BAC B30-MT MATERIAL STEEL H11
NUT BAC N10-MT HEAT TREAT 220 KSI

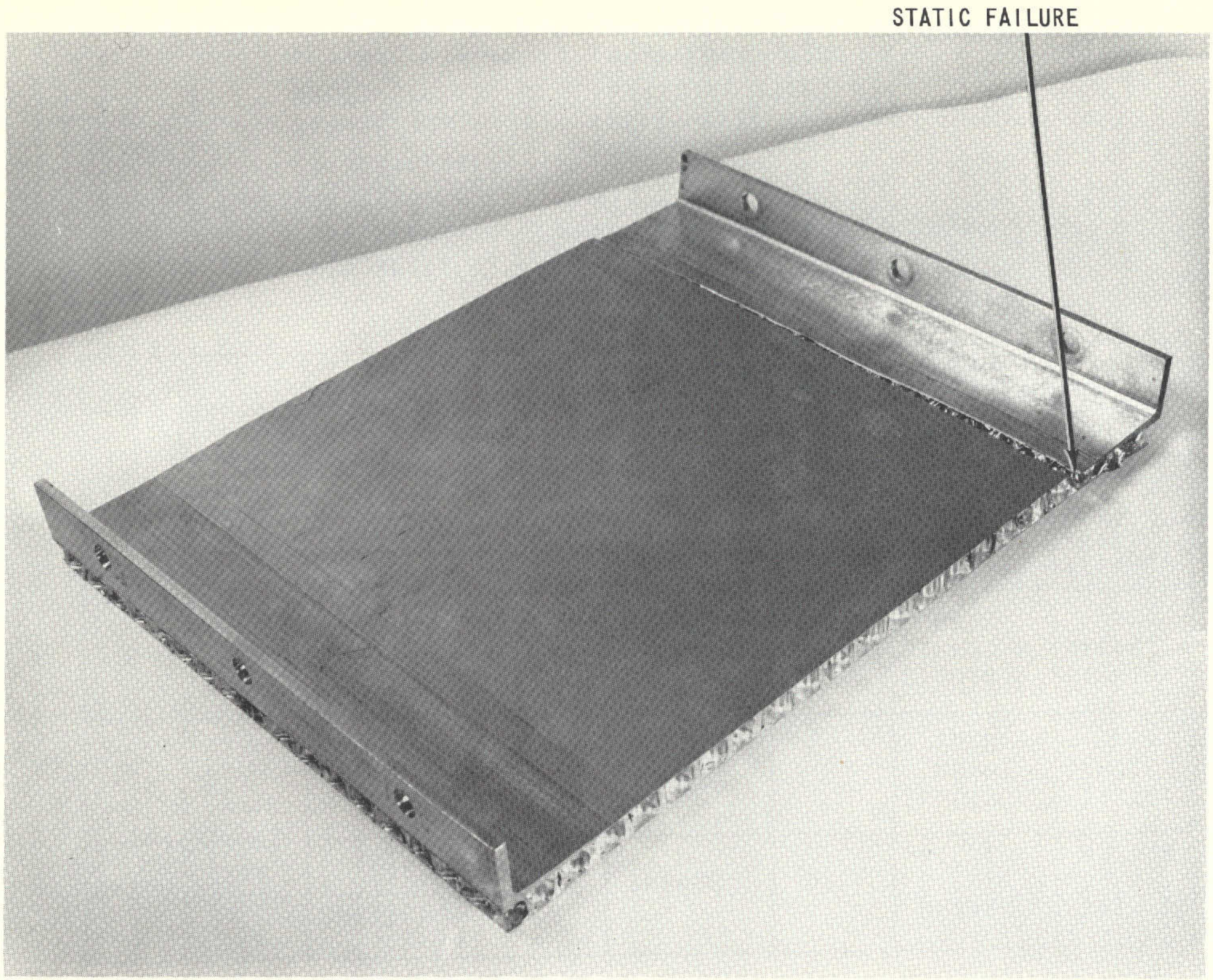

FIGURE 2. TYPICAL FLANGE PANEL

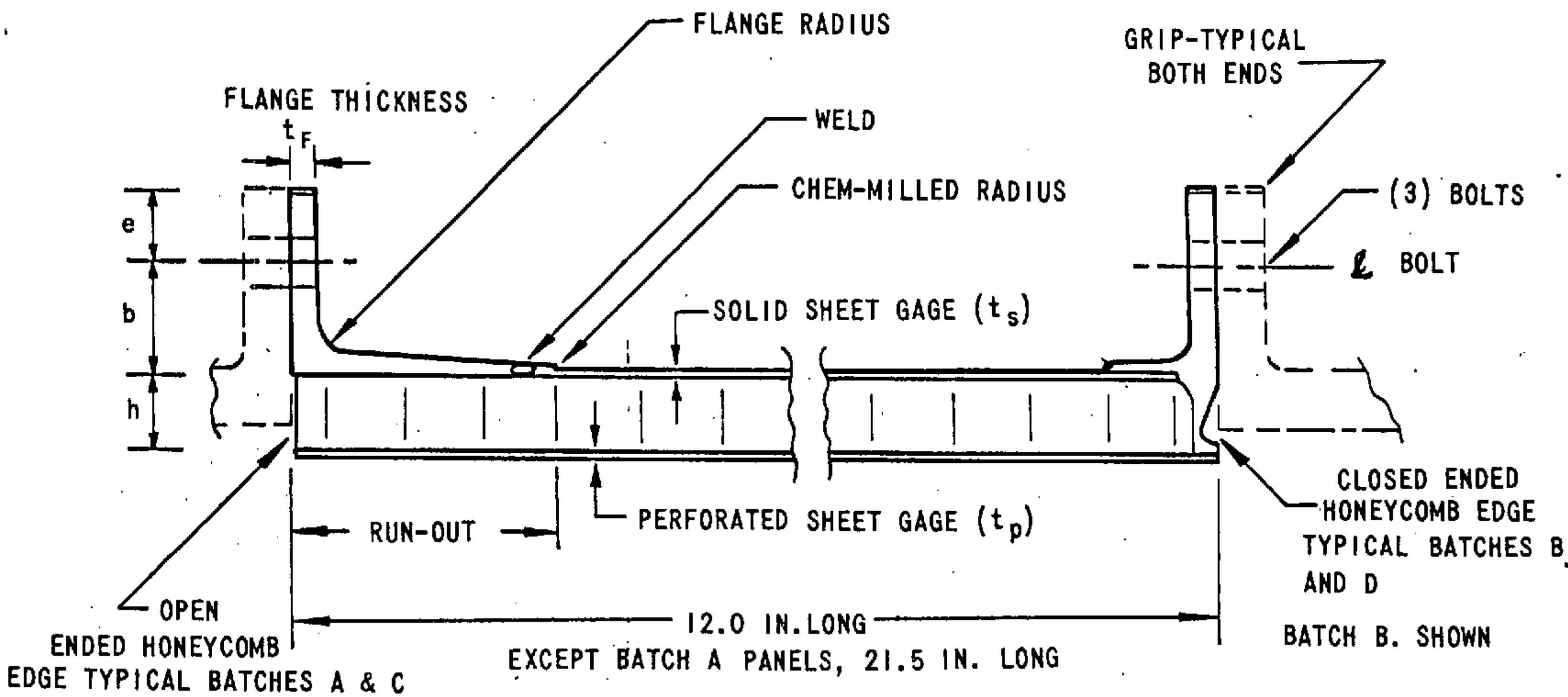

FIGURE 3. CONFIGURATION OF FLANGE PANELS

TABLE 2 - FLANGE PANEL DIMENSIONS

TEST NO.	BATCH	PANEL WIDTH W	FLANGE ATTACHMENT BOLTS 3 PER FLANGE			CORE TYPE	CORE DEPTH h	FLANGE THICKNESS t_f	SOLID SKIN t_s	PERFORATED SKIN t_p
			BOLT DIAMETER	e	b					
1	A	7.0	0.25	0.40	0.60	4-25	0.25	0.16	0.013	0.016
2	A									
3	A									
4	B	7.0	0.25	0.40	0.60	4-25	0.50	0.15	0.013	0.013
5	B									
6	B									
7	B									
8	C	9.0	0.3125	0.40	0.60	6-20	0.375	0.15	0.013	0.016
9	C		0.3125							
10	C		0.25							
11	C		0.3125							
12	D	9.0	0.3125	0.40	0.60	6-35	0.50	0.16	0.013	0.013
13	D	7.0	0.25							
14	D	7.0	0.25							
15	D	9.0	0.25							

DIMENSIONS IN INCHES
TESTS 1, 4, 8 AND 12 STATIC TEST.
BATCHES A AND C OPEN CORE FLANGE
B AND D CLOSED CORE FLANGE
BATCH A 21.5 INCHES LONG. BATCHES B, C, AND D - 12.0 INCHES LONG
HOLE DIA. 1/4 DIA. BOLT = .28 IN. 5/16 DIA. BOLT = .35 IN.

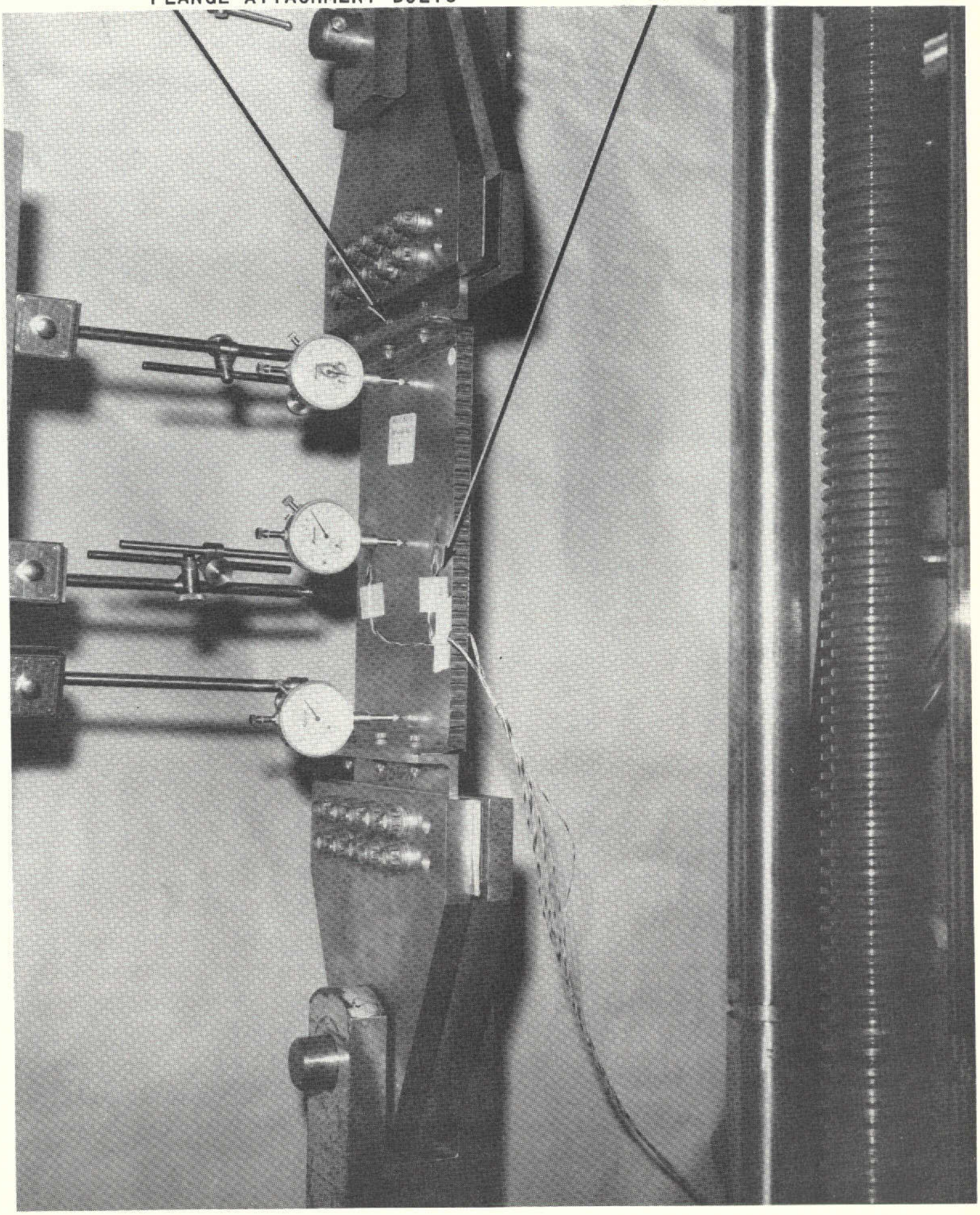

FIGURE 4. TYPICAL FLANGE PANEL IN TEST FIXTURE - BATCH B PANEL SHOWN

TABLE 3 - FLANGE PANEL STATIC TEST RESULTS

TEST NO.	BATCH	APPLIED LOAD P LB.	FAILURE DESCRIPTION
1	A	13,800	FAILED AT CHEM-MILLED RADIUS - CENTER BOLT FAILED.
4	B	10,680	FAILED AT CHEM-MILLED RADIUS - 2 BOLTS FAILED.
8	C	19,650	FAILED AT CHEM-MILLED RADIUS - 2 BOLTS AT THREADS AND NUT PLATE STRAP ALSO FAILED.
12	D	18,600	FAILED AT CHEM-MILLED RADIUS IN FACE SHEET.

DESIGN LOAD FOR PANELS ULTIMATE

TEST NUMBER 1, 4	7.0 INCH WIDE PANELS	8,925 LB.
8, 12.	9.0 INCH WIDE PANELS	11,470 LB.

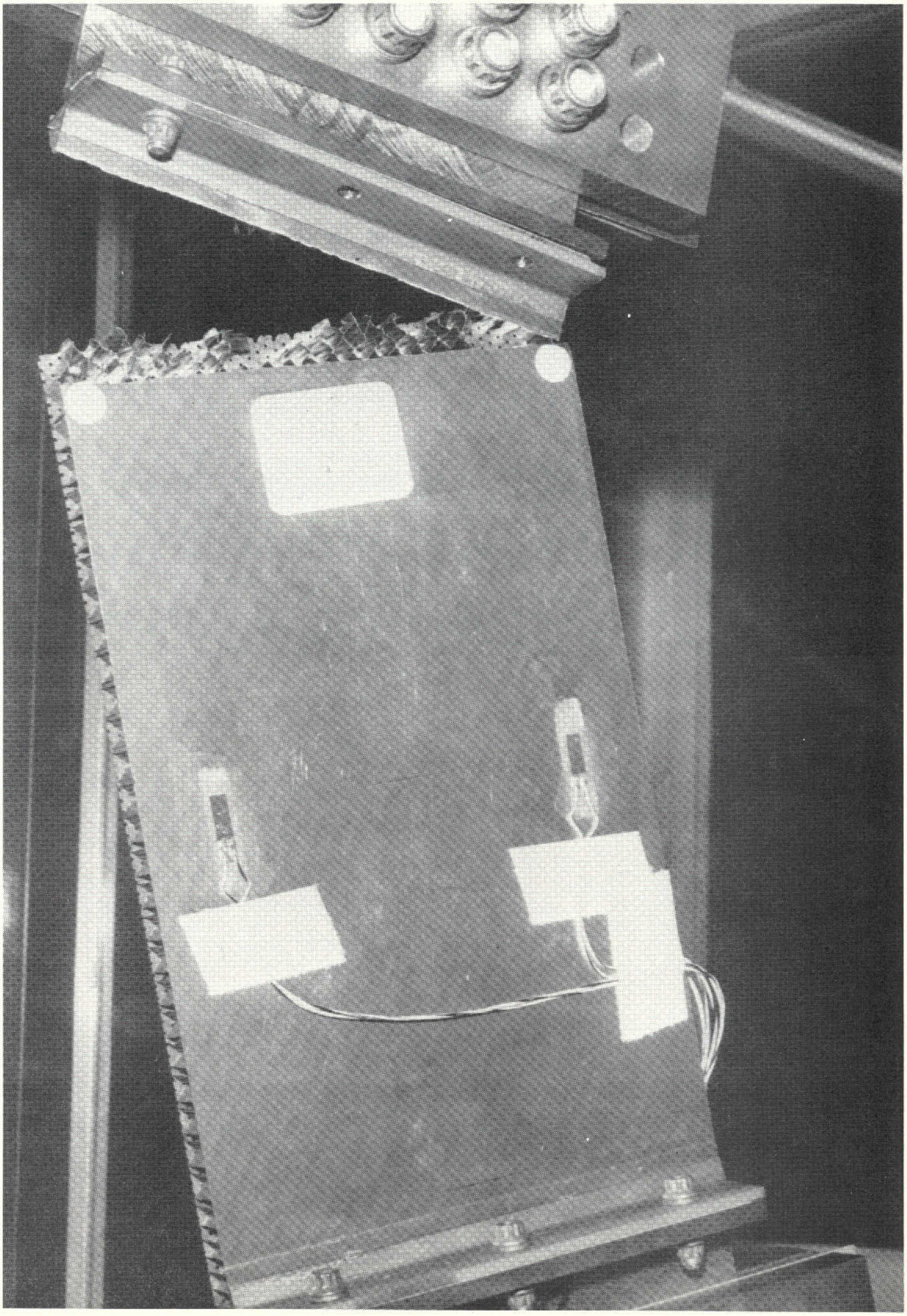

FIGURE 5. TYPICAL FLANGE PANEL STATIC FAILURE

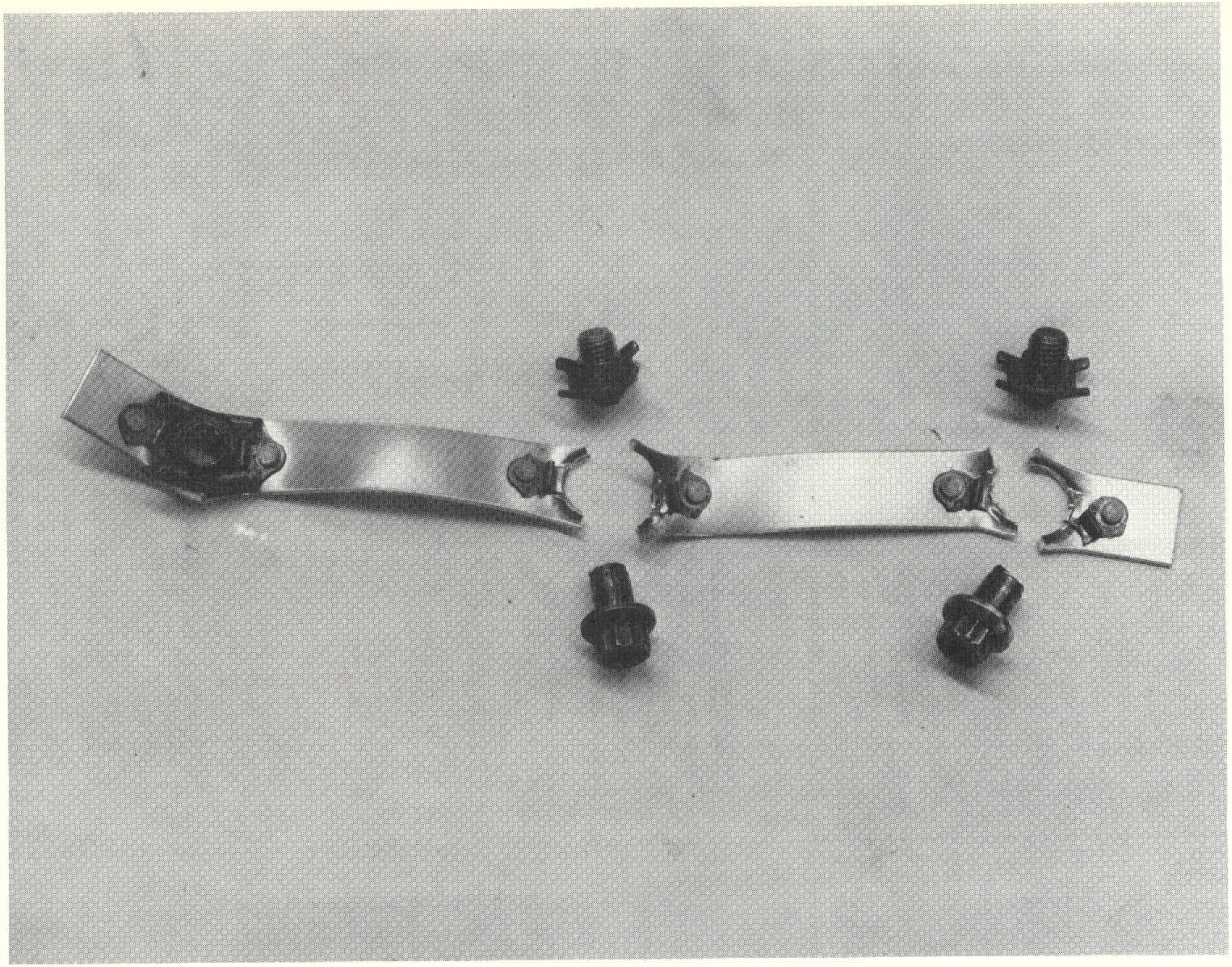

FIGURE 6. NUT PLATE STRAP STATIC FAILURE

TABLE 4 - FLANGE PANEL FATIGUE TEST RESULTS

TEST NO.	BATCH	APPLIED LOAD P LB.	STRESS RATIO R	NO. OF CYCLES TO FAILURE	EQUIVALENT CYCLES P = 3150LB R=0.10	FAILURE DESCRIPTION
2	A	3,750	0.060	80,000	200,000	UNSUPPORTED DOUBLE SETUP MULTIPLE FAILURES AT BOLT HOLES
3	A	3,750	0.06	52,000 192,000	480,000	BOLT FAILURES:SUPPORTED DOUBLE PANEL SETUP BOLT FAILURE CRACKS IN CHEM-MILLED RADIUS OF SKIN FLANGE CRACKED AT BOLT HOLES
5	B	3,500	0.10	34,000 47,000	73,000	BOLT FAILURE BOLT FAILURE PANEL FAILED AT JUNCTION WITH EDGE MEMBER
6	B	3,000	0.10	56,000 76,000	61,000	BOLT FAILURE PANEL FAILED AT JUNCTION WITH EDGE MEMBER
7	B	2,500	0.10	201,000	78,000	PANEL FAILED AT JUNCTION WITH EDGE MEMBER FLANGE CRACKED AT BOLT HOLE
9	C	4,500 3,900	0.10	33,000 50,000 83,000 503,000	$13x10^6$	BOLT FAILURE LOAD REDUCED TO 3900 LB. BOLT FAILURE BOLT FAILURE:REPLACED WITH LONG BOLTS CRACKS AT FLANGE RADIUS FLANGE CRACKS AT BOLT HOLES
10	C	4,500	0.10	8,000		3 BOLTS FAILED PANEL DAMAGED FATIGUE TEST TERMINATED
11*	C	3,900 4,500	0.10	$1.007x10^6$ $1.455x10^6$	$4.76x10^6$	LOAD INCREASED FROM 3900 TO 4500 LB. BOLT FAILED FLANGE CRACKS AT BOLT HOLES
13*	D	3,000 3,500	0.10	500,000 511,000	420,000	LOAD INCREASED TO 3500 LB CRACK IN SOLID SKIN AT PANEL CENTER
14*	D	3,500	0.10	77,000	120,000	CRACK IN WELD
15*	D	3,900	0.10	148,000	370,000	MULTIPLE CRACKS IN WELD

* NOTE: LONG BOLTS AND STACKED WASHERS USED IN TESTS 11, 13, 14, 15

TYPICAL STATIC TEST FAILURE AT SKIN CHEM-MILLED RADIUS

TEST NO. 9 FAILURE IN FLANGE AND AT BOLT HOLES

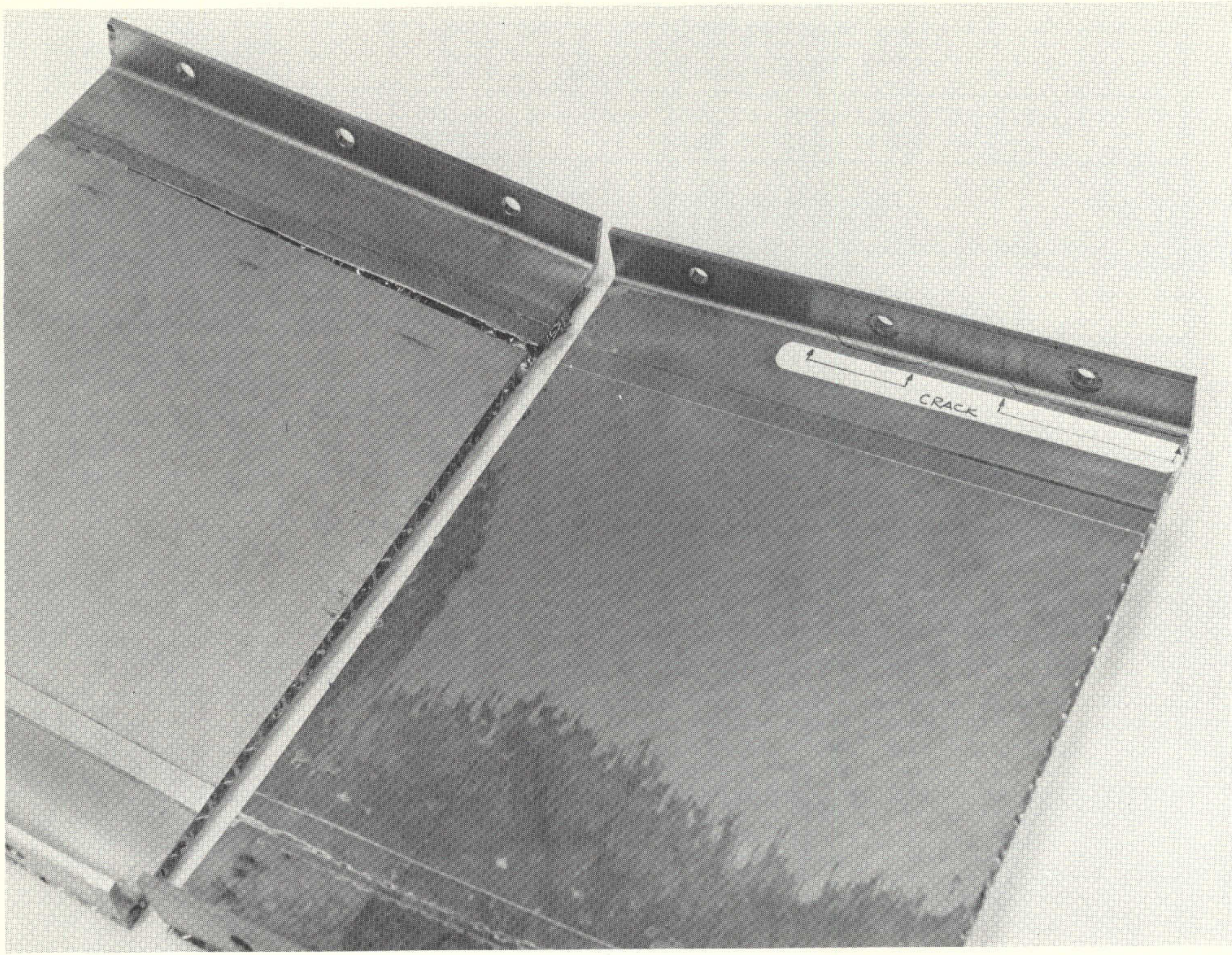

FIGURE 7. TYPICAL STATIC AND FATIGUE TEST FLANGE PANEL FAILURES

TEST NO. 14 PANEL
FAILURE IN WELD

TEST NO. 13 PANEL
SKIN FAILURE

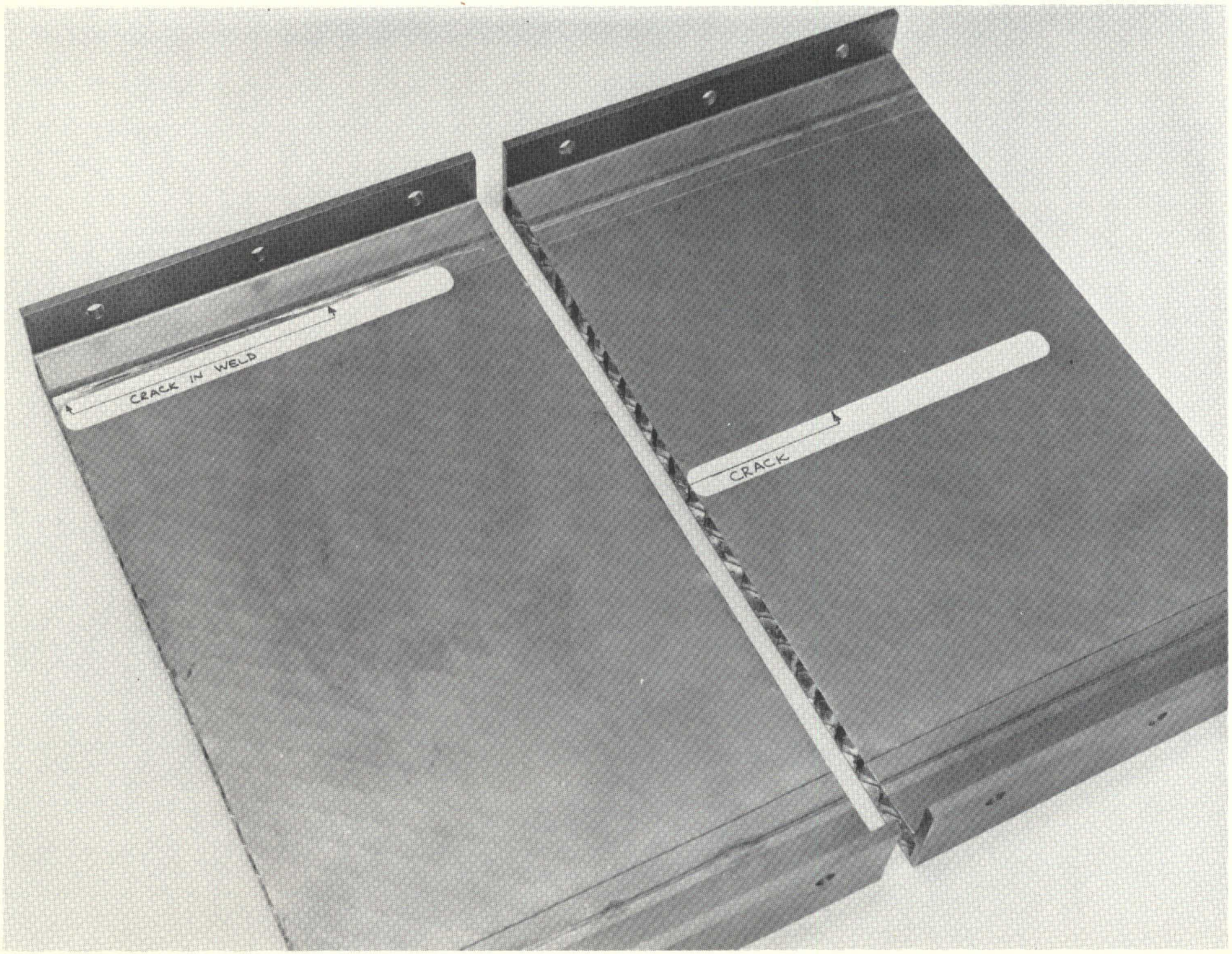

FIGURE 8. TYPICAL FLANGE PANEL FAILURES — FATIGUE TEST

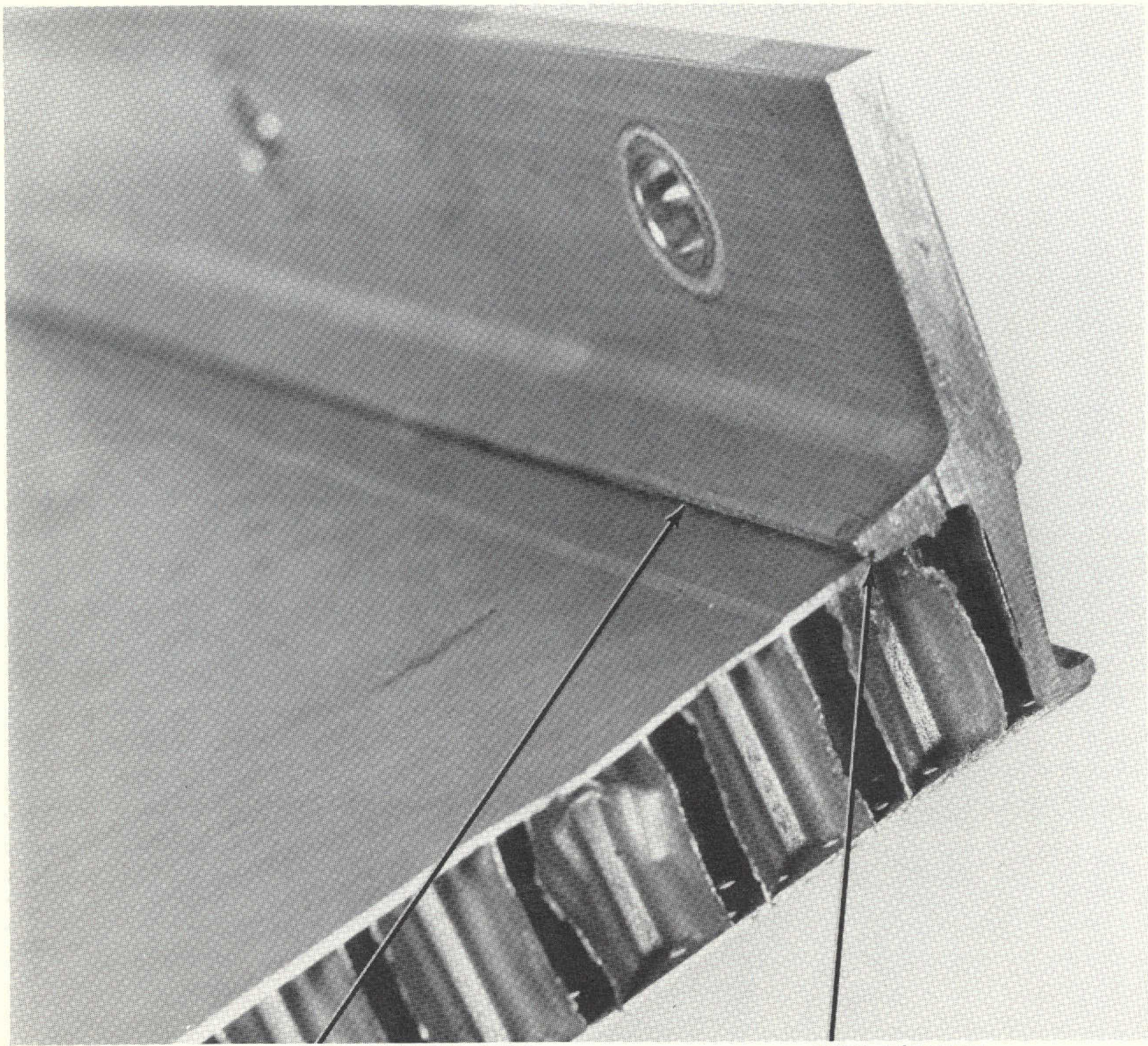

FIGURE 9. BATCH B PANEL SHOWING FAILURE OF SKIN DUE TO HIGH STRESS CONCENTRATION

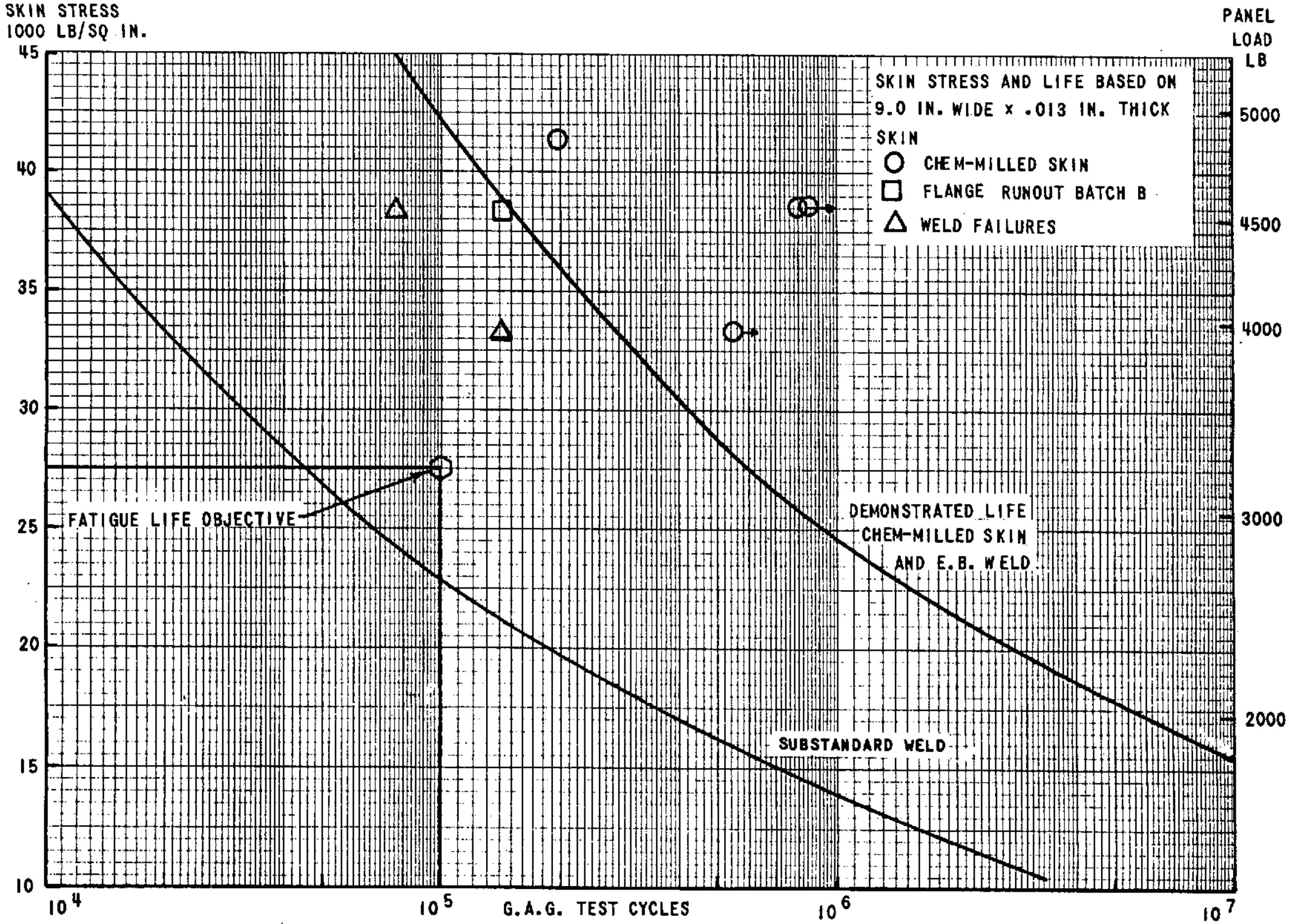

FIGURE 10. FLANGE PANEL SKIN AND WELD FATIGUE LIFE CURVE

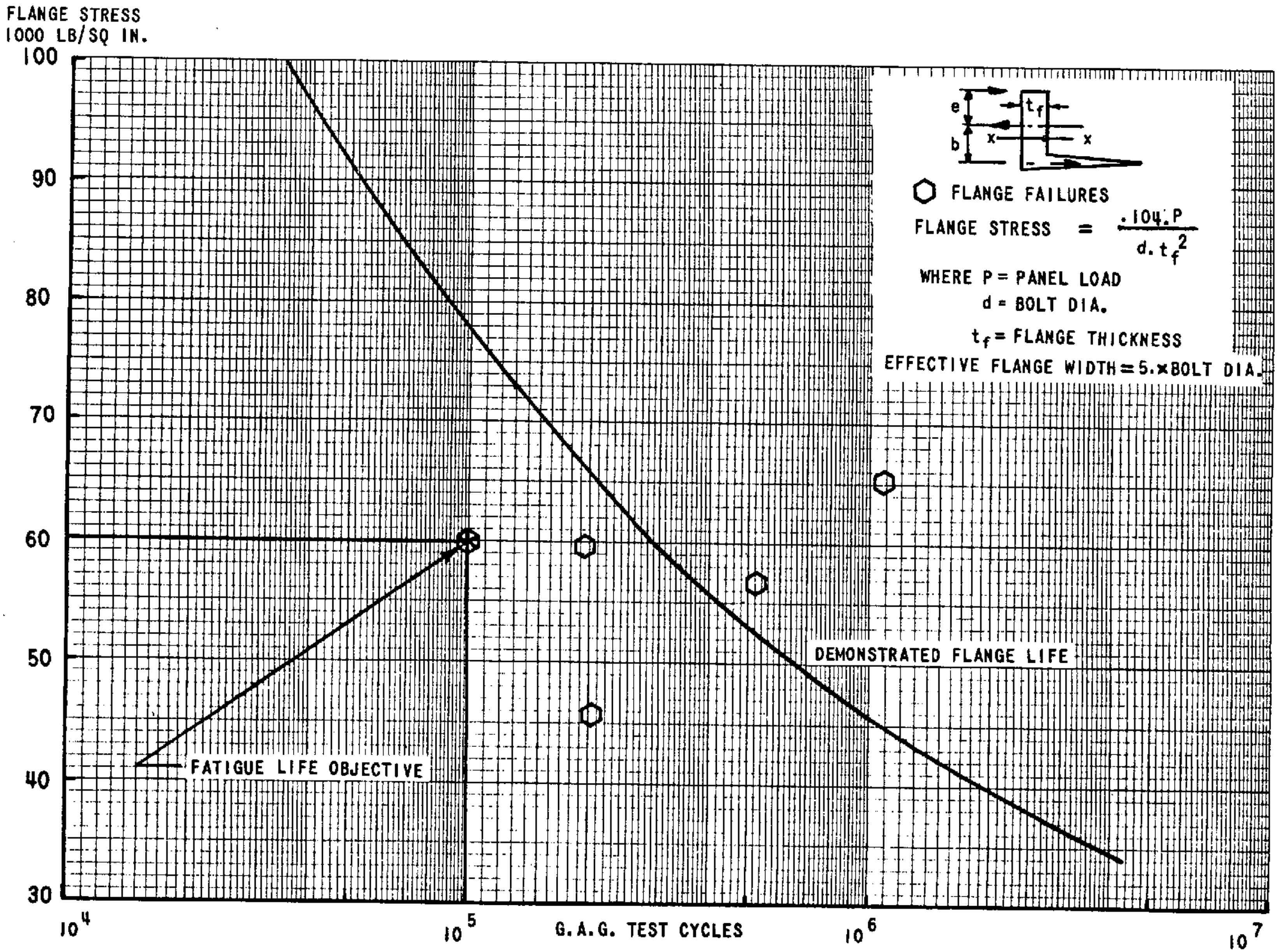

FIGURE 11. FLANGE PANEL - FLANGE LIFE CURVE

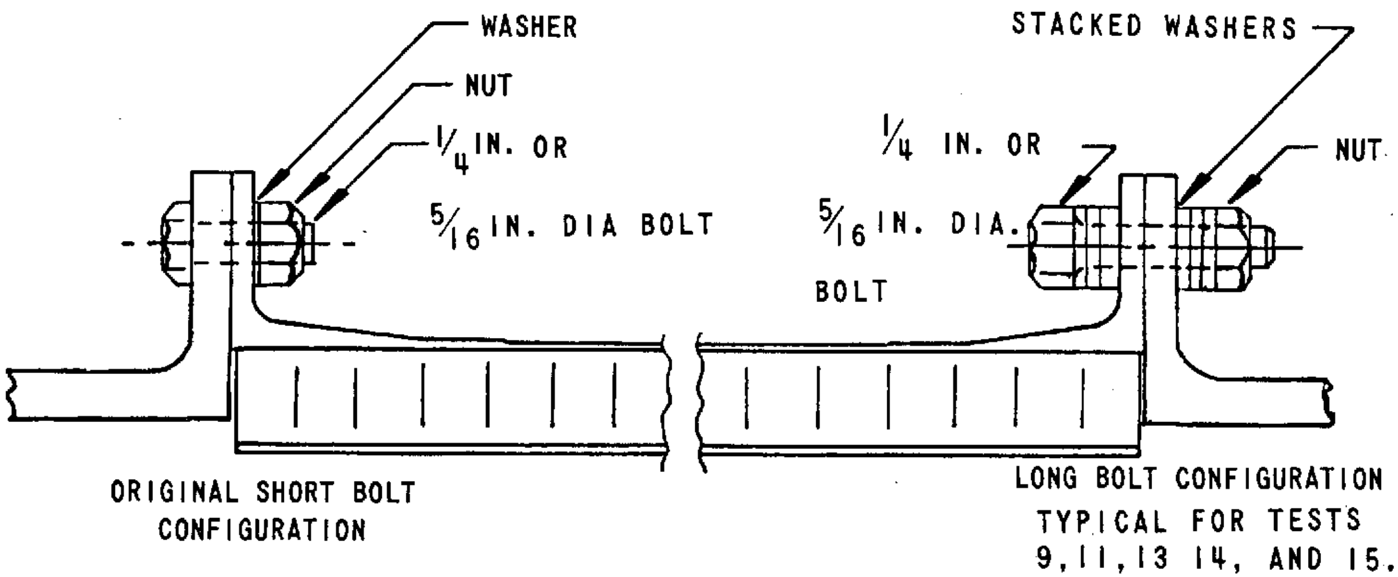

FIGURE 12. CONFIGURATION OF FLANGE PANEL ATTACHMENT BOLTS

TABLE 5. FLANGE PANEL TEST—BOLT FAILURE SUMMARY.

TEST NO.	BOLT BAC B30	DIA. IN.	TORQUE IN. LB.	APPLIED LOAD P	STRESS RATIO	NO. OF CYCLES TO FAILURE	FAILURE DESCRIPTION
2	MT 4-7	1/4	90-125	3,750	.06	80,000	MULTIPLE CRACKS IN FLANGES AT BOLT HOLES.
3	MT 4-7	1/4	90-125	3,750	.06	52,000	BOLT FAILED CENTER LWR. ALL BOLTS REPLACED.
	MT 4-7	1/4	90-125			144,000	SAME BOLT FAILED. BOLT REPLACED.
						191,000	NO BOLT FAILURES. PANEL FAILURE.
5	MT 4-7	1/4	90-125	3,500	.10	34,000	BOLT FAILED CTR. UPPER IN THREADS REPLACED WITH NUT ON FIXTURE SIDE.
	MT 4-7	1/4	90-125			47,000	SAME BOLT FAILED. UPPER HEAD ALL BOLTS REPLACED. HEADS ON FIXTURE SIDE, SELF ALIGNING WASHER UNDER NUT.
						49,000	PANEL FAILED. NO BOLT FAILURE.
6	MT 4-7	1/4	90-125	3,000	.10	56,000	BOLT FAILED UPPER RH BOLT REPLACED HEAD ON FIXTURE SIDE.
						76,000	BOLT FAILED UPPER LH SIDE. PANEL FAILURE
7	MT 4-7	1/4	90-125	2,500	.10	201,000	NO BOLT FAILURES. PANEL FAILURE.
9	MT 5-7	5/16	90-125	4,500	.10	33,000	BOLT FAILED UNDER HEAD LWR. CTR. FIXTURE SIDE. REPLACED WITH NUT ON FIXTURE SIDE. LOAD REDUCED TO 3,900 LB.
	MT 5-7	5/16	90-125	3,900	.10	50,000	2 BOLTS FAILED UNDER HEADS UPR. CTR. & R.H. FIXTURE SIDE. REPLACED WITH NUT ON FIXTURE SIDE.
				3,900	.10	83,000	SAME 2 BOLTS FAILED UNDER HEADS UPPER CTR. & R.H. FLANGE SIDE.
	MT 5-11 STACKED WASHERS	5/16	250	3,900	.10		ALL 6 BOLTS REPLACED WITH LONG BOLTS. HEADS ON FIXTURE SIDE. FLAT & SELF ALIGNING WASHERS USED TO ACCOMMODATE EXTRA LENGTHS UNDER HEAD AND NUT.
				3,900	.10	503,000	NO BOLT FAILURES. PANEL FAILURE.
10	MT 4-7	1/4	90-120	4,500	.10	8,000	3 BOLTS FAILED UNDER HEADS. LOWER FLANGE. FIXTURE SIDE PANEL DAMAGED. TEST TERMINATED.
11	MT 5-11 STACKED WASHERS	5/16	250	3,900	.10	1,007,000	NO FAILURES. FLAT AND SELF ALIGNING WASHERS USED UNDER HEAD & NUT. LOAD INCREASED TO 4500 LB.
				4,500	.10	1,455,000	BOLT FAILED IN THREAD. LWR. LH. PANEL SIDE. PANEL FLANGE CRACKED.
13	MT 4-12	1/4	175-185	3,000	.10	500,000	HEAD ON FIXTURE SIDE. FLAT AND SELF ALIGNING WASHERS USED UNDER HEAD & NUT. LOAD INCREASED TO 3500 LB.
				3,500		511,000	PANEL FAILED. NO BOLT FAILURES.
14	MT 4-12	1/4	175-185	3,500	.10	77,000	PANEL FAILED. NO BOLT FAILURES.
15	MT 4-12	1/4	175-185	3,900	.10	148,000	PANEL FAILED. NO BOLT FAILURES.

BOLT USED BAC B30 MT - MATERIAL STEEL H11. HEAT TREAT. F_{TU} 220 KSI. F_{SU} 125 KSI.

NUT USED BAC N10 HR.;

BOLT PRELOAD STRESS
1/4 IN. DIA. 90-125 IN.LB. = 70,000 LB/SQ.IN.
1/4 IN. DIA. 175-185 IN.LB.= 120,000 LB/SQ.IN.
5/16 IN. DIA. 250 IN.LB. = 70,000 LB/SQ.IN.

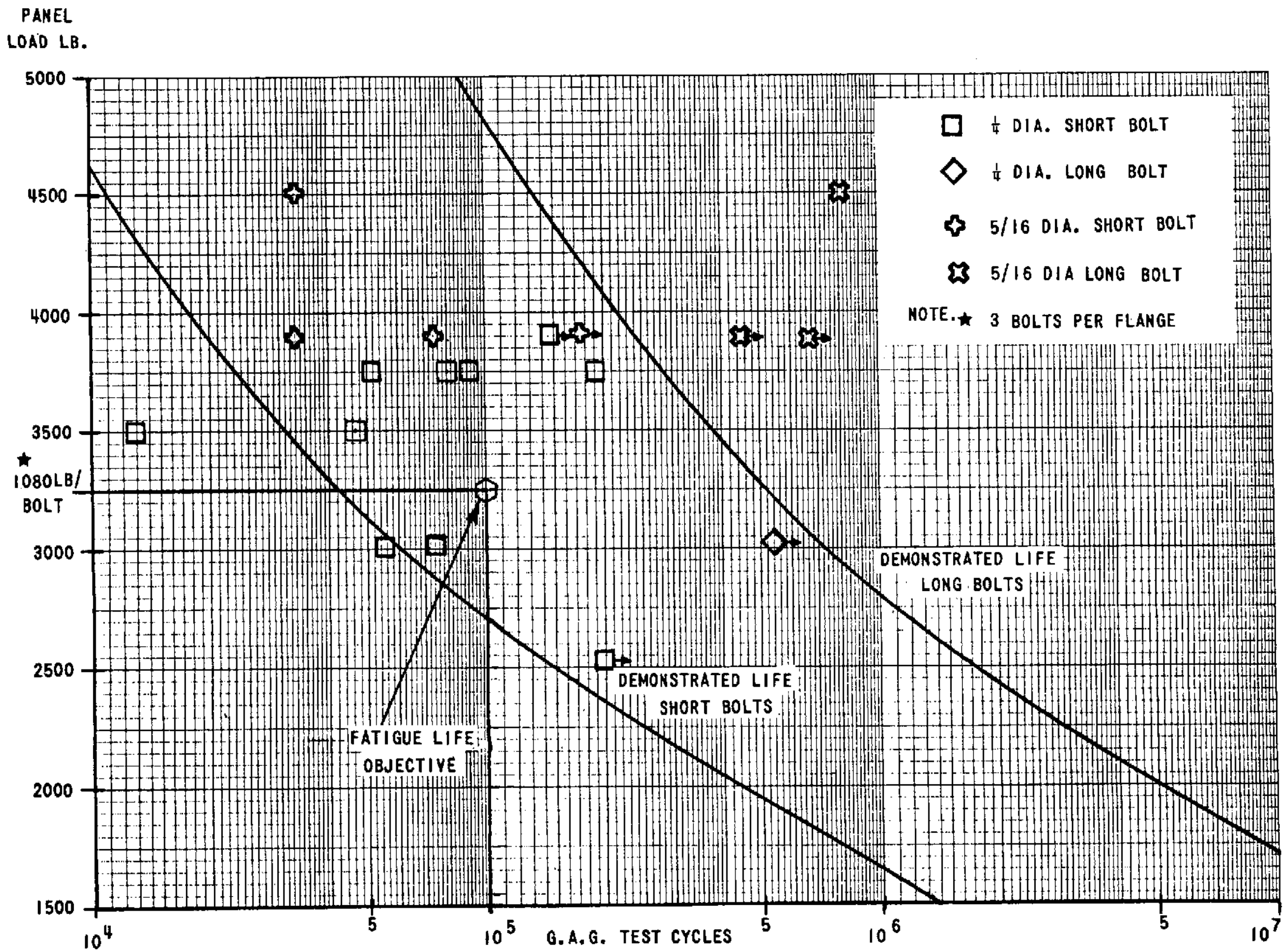

FIGURE 13. FLANGE PANEL TEST - BOLT LIFE CURVE

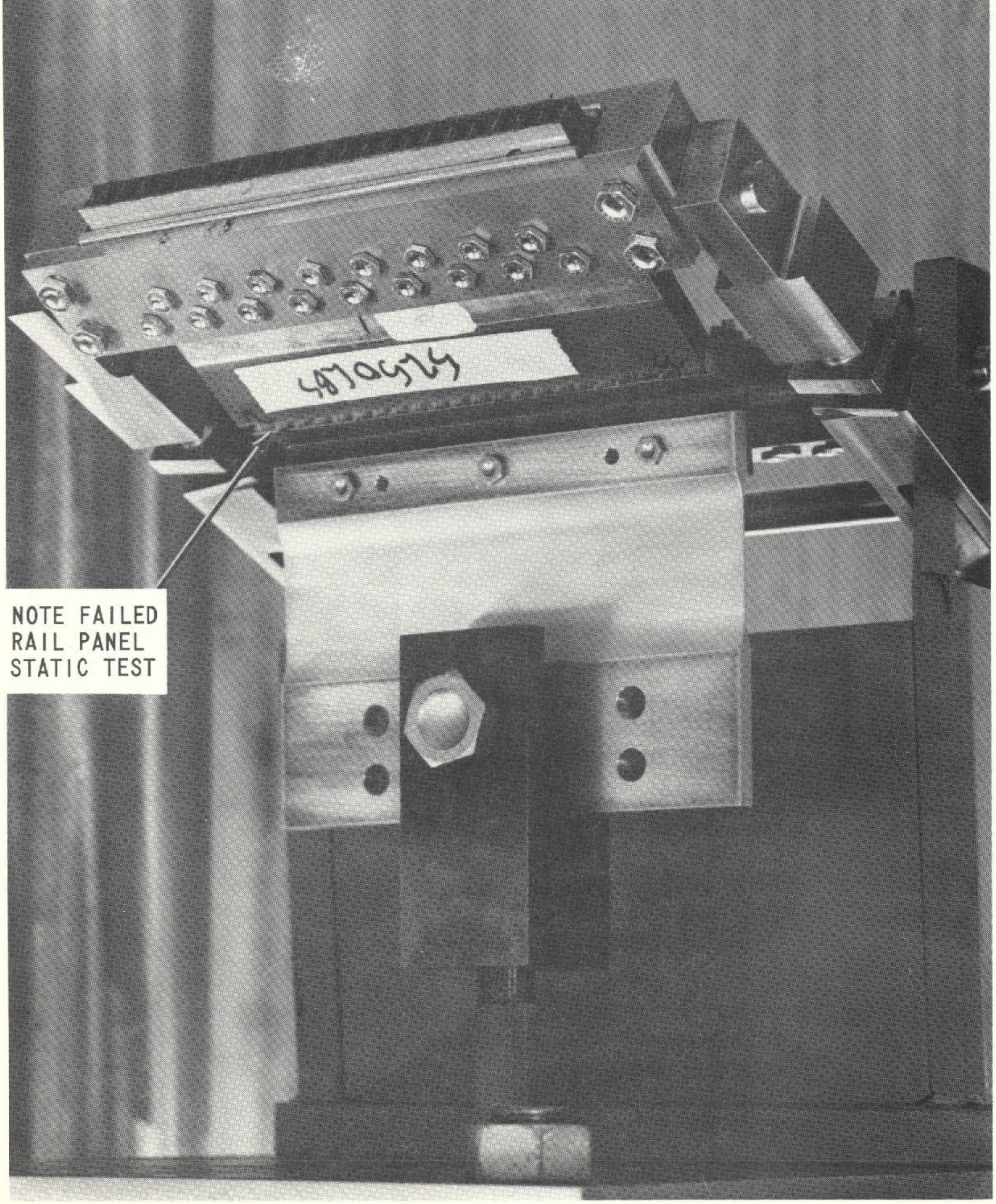

FIGURE 14. TYPICAL RAIL PANEL IN TEST FIXTURE

TABLE 6 - RAIL PANEL DIMENSIONS

TEST NO.	BATCH	PANEL WIDTH W	CORE TYPE	CORE DEPTH h	SOLID SKIN t_s	PERF'D SKIN t_p	RAIL GAGE t_r
1&2 3&4	B	9.0	4-25	0.50	0.013	0.013	0.15
5&6 7&8	C	9.0	6-20	0.375	0.013	0.016	0.15
9&10 11&12	D	7.0 9.0	6-35	0.50	0.013	0.013	0.15

DIMENSIONS IN INCHES
TESTS 1,5,9 STATIC TESTS

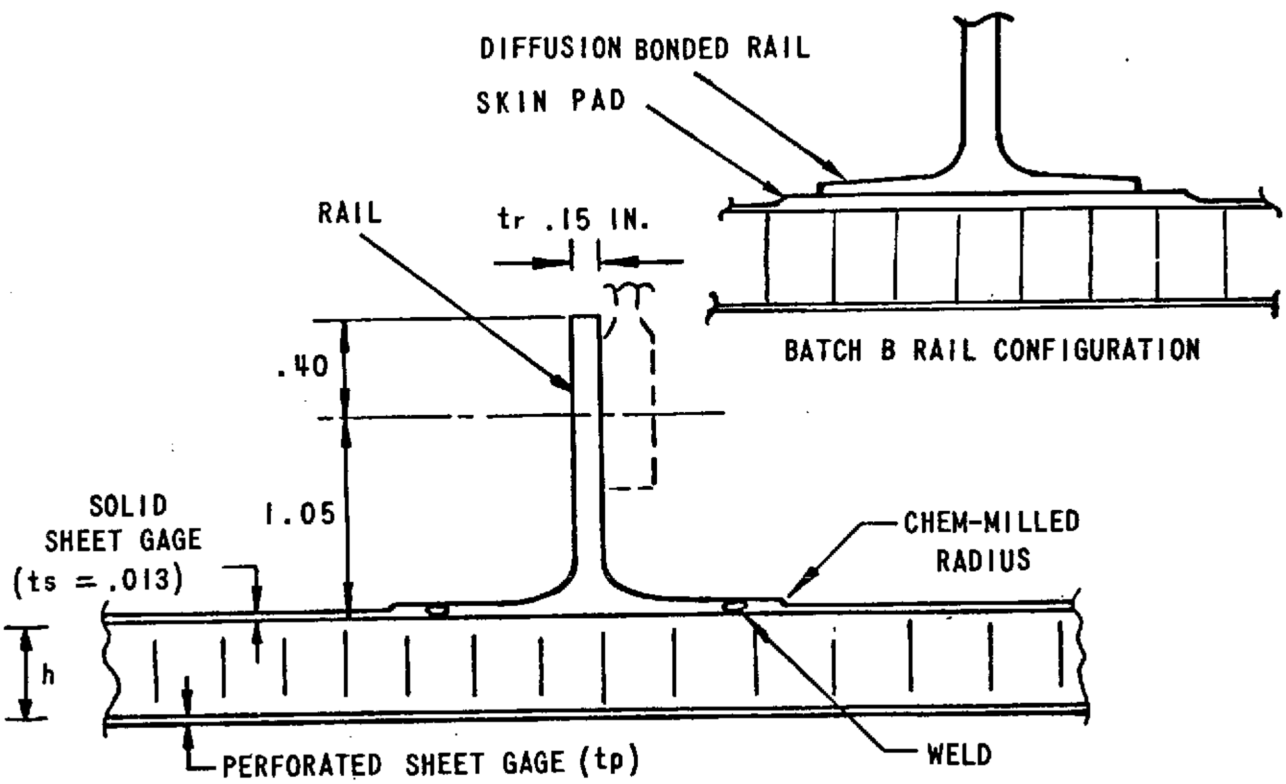

FIGURE 15. CONFIGURATION OF RAIL PANELS

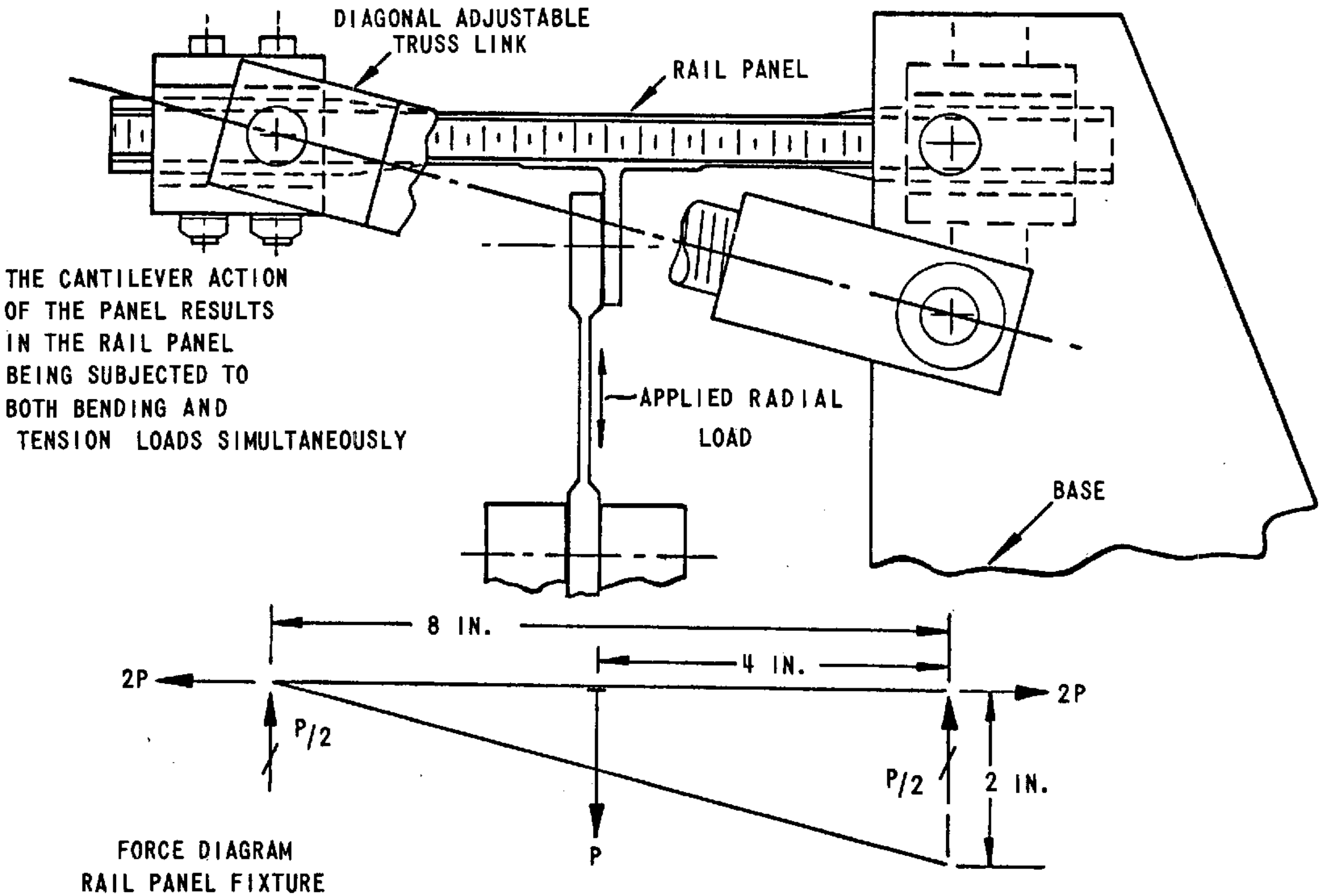

FIGURE 16. RAIL PANEL LOADING DIAGRAM

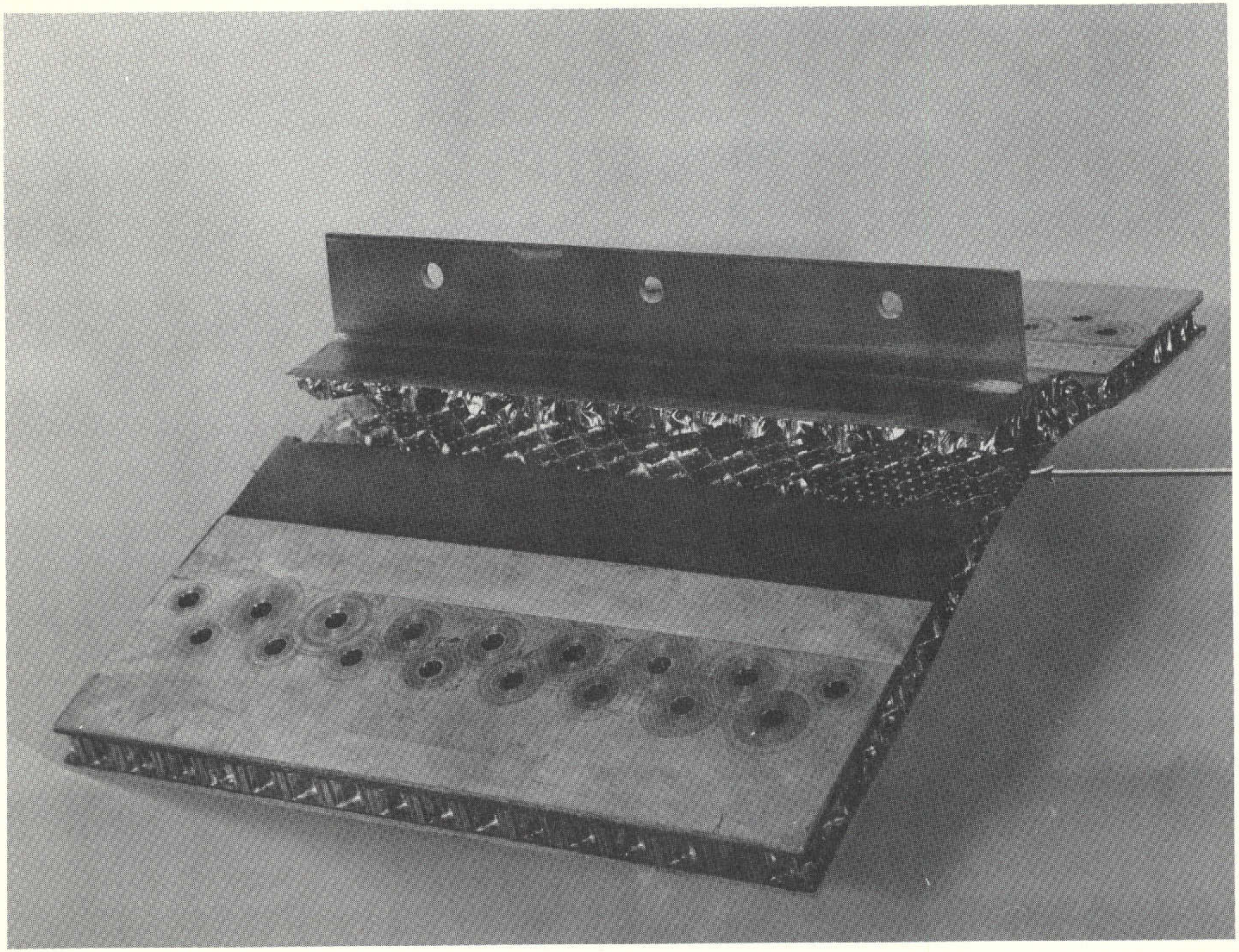

FIGURE 17. RAIL PANEL STATIC FAILURE

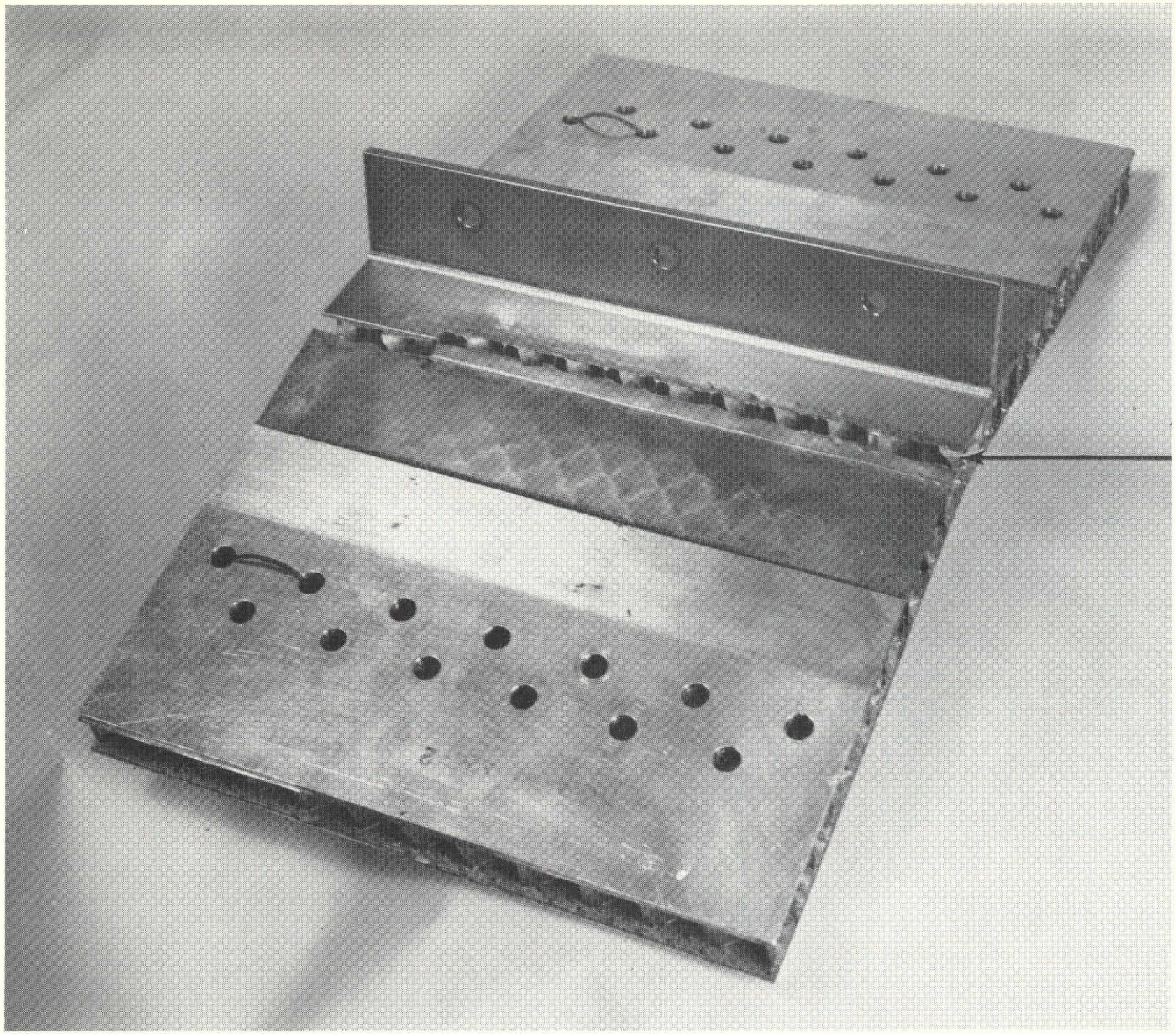

FIGURE 18. RAIL PANEL STATIC FAILURE

TABLE 7 - RAIL PANEL STATIC TEST RESULTS

TEST NO.	BATCH	APPLIED LOAD P LB.	FAILURE DESCRIPTION
1	B	5,250	FAILED AT CHEM-MILLED RADIUS IN SOLID SHEET
5	C	13,450	FAILED AT CHEM-MILLED RADIUS IN SOLID SHEET CORESHEAR FAILURE AT 6000 LB
9	D	2,800	FAILED AT WELD AND SOLID SKIN

DESIGN LOAD FOR RAIL PANELS ULTIMATE

TEST No. 9 7.0 INCH WIDE PANEL 2700 LB.

1, 5 9.0 INCH WIDE PANEL 3500 LB.

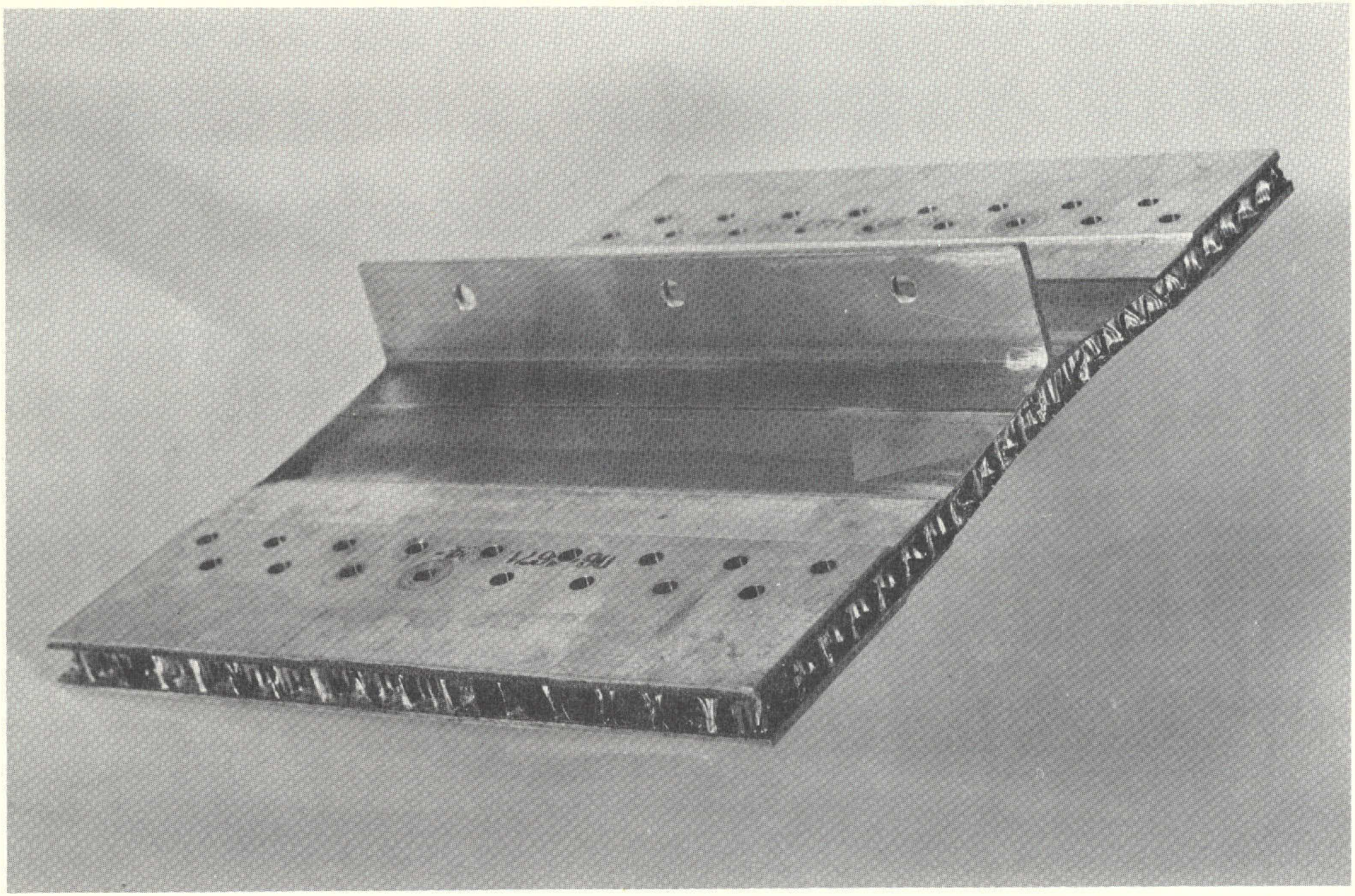

PANEL DEFORMED DUE TO CORE SHEAR FAILURE. TYPICAL OF TESTS 6, 7 AND 8

FIGURE 19. RAIL PANEL FATIGUE FAILURE

PANEL CRACKED IN SKIN

PANEL CRACKED AT WELD REPAIR

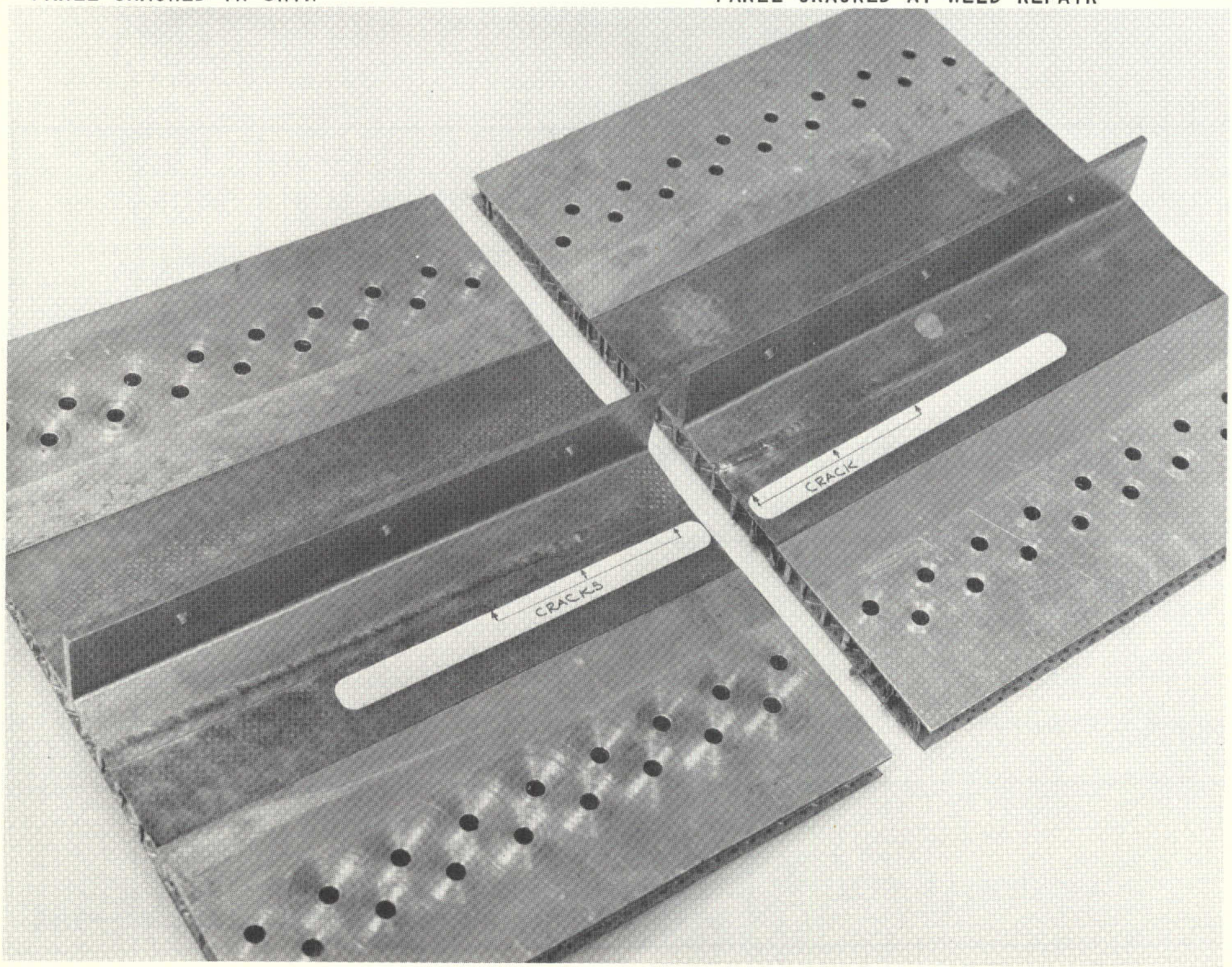

FIGURE 20. RAIL PANEL FATIGUE FAILURE

TABLE 8 - RAIL PANEL.FATIGUE TEST RESULTS

TEST NO.	BATCH	APPLIED LOAD LB. P	STRESS RATIO R	NO. OF CYCLES TO FAILURE	EQUIVALENT CYCLES LOAD = 1400 LB R= 0.10	FAILURE DESCRIPTION
2	B	1,600	0.10	351,000	597,000	SOLID SKIN CRACK 1/4 INC. FROM CHEM. MILLED RADIUS
3		2,000	0.10	132,000	660,000	SOLID SKIN 1/4 IN. FROM CHEM. MILLED RADIUS.
4		2,400	0.10	31,000	372,000	CORE FAILURE IN SHEAR, BUCKLED PERFORATED SKIN.
6	C	2,400	0.10	6,000	72,000	CORE FAILED IN SHEAR. 6-20 CORE
7		1,600	0.10	6,000	10,000	AS TEST 6
8		800	0.10	61,000	5,700	AS TEST 6
10	D	1,200	0.10	231,000	130,000	SOLID SKIN AT WELD
11		1,400	o.10	353,000	353,000	SOLID SKIN AT WELD
12		1,600	0.10	107,000	182,000	SOLID SKIN AT WELD. CORE NOISE AUDIBLE.

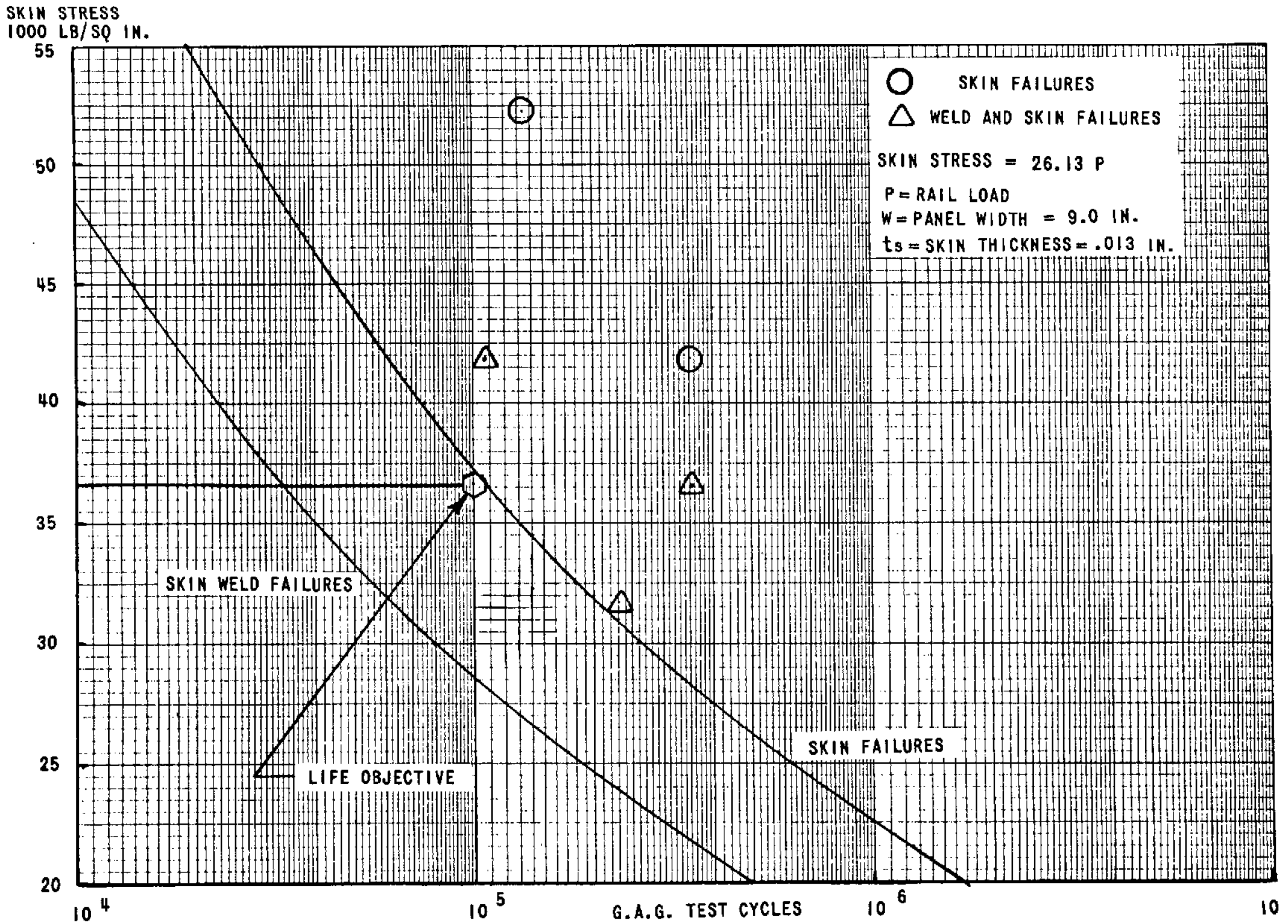

FIGURE 21. RAIL PANEL SKIN AND WELD FATIGUE LIFE CURVE

TABLE 9. SHEAR SPECIMEN DIMENSIONS

TEST NO.	BATCH	CORE	CORE DEPTH h	LENGTH L	WIDTH W	SOLID SKIN t_s	PERF'D SKIN t_p
1 2	B	4-25	0.50	2.0	2.0	0.013	0.013
3 4	C	6-20	0.375	2.25	2.0	0.013	0.016
5 6 7 8	D	6-35	0.50	2.0	2.0	0.013	0.013

DIMENSIONS IN INCHES   TESTS 1 AND 5 STATIC TEST

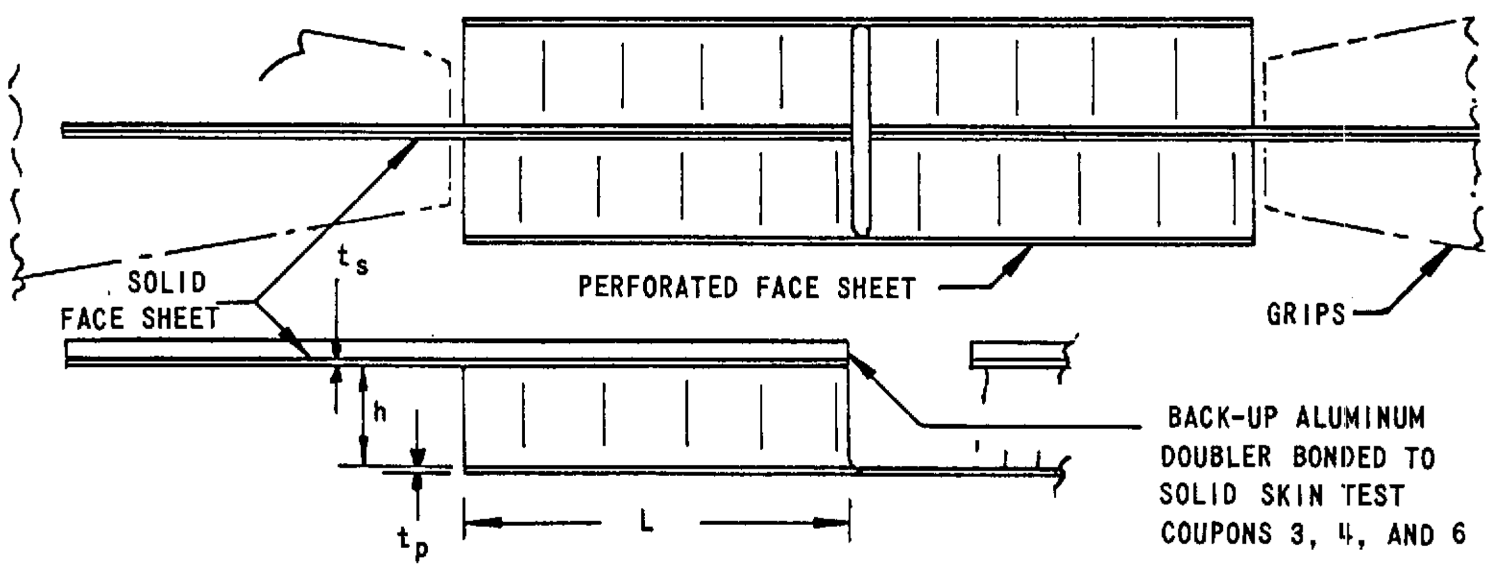

FIGURE 22. SHEAR SPECIMEN SHOWING BACK TO BACK MOUNTING AND BONDED SKIN REINFORCING DOUBLER

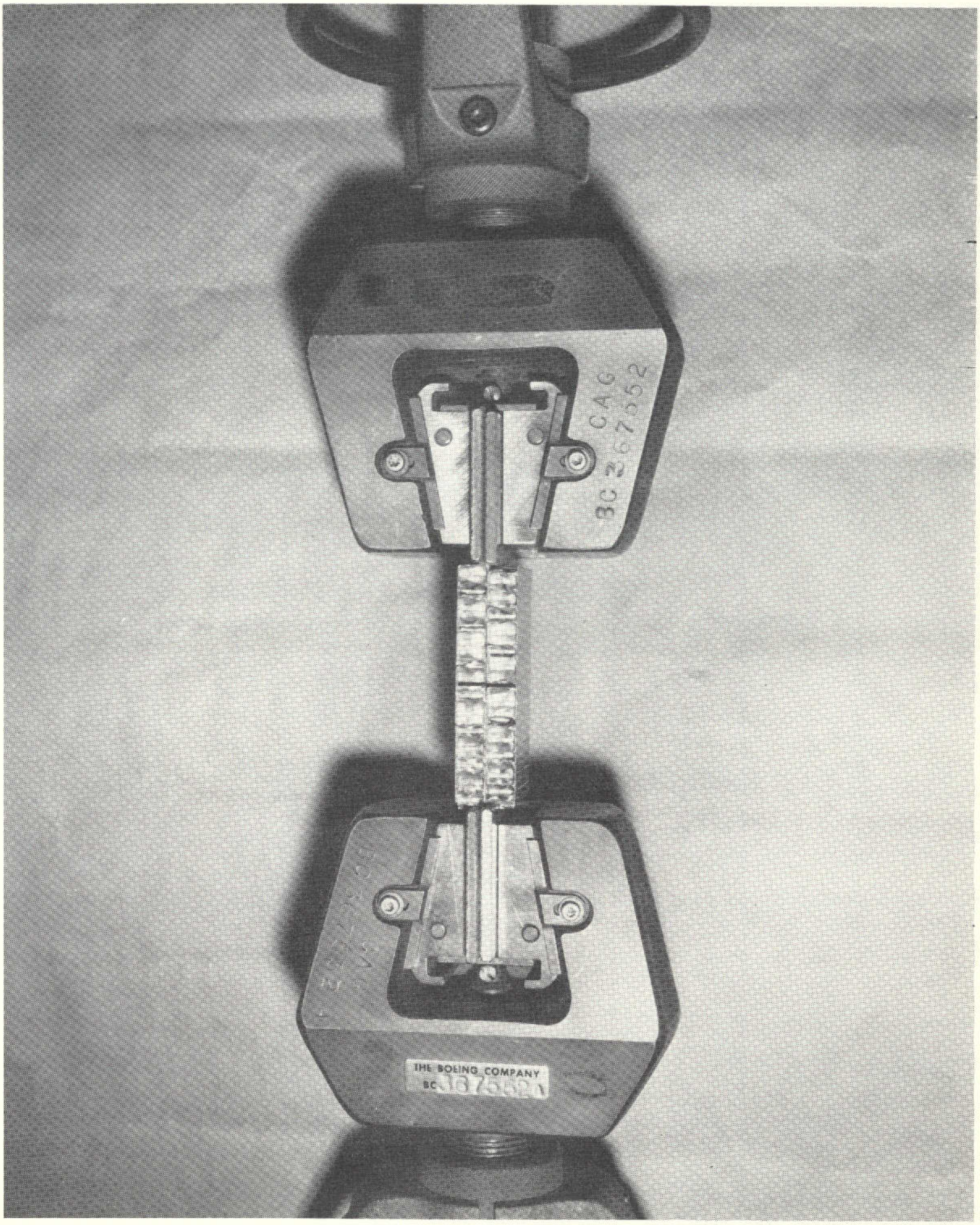

FIGURE 23. SHEAR SPECIMEN STATIC TEST SET UP - COUPONS MOUNTED BACK TO BACK

TABLE 10. SHEAR SPECIMEN STATIC TEST RESULTS

TEST NO.	BATCH	APPLIED LOAD LB. P	FAILURE DESCRIPTION
1	B	2,580	BOND FAILURE
5	D	2,455	CORE AND BRAZE FAILURE

DESIGN LOAD FOR SHEAR COUPONS ULTIMATE 1680 LB.
SKIN NOT BACKED UP WITH DOUBLERS.

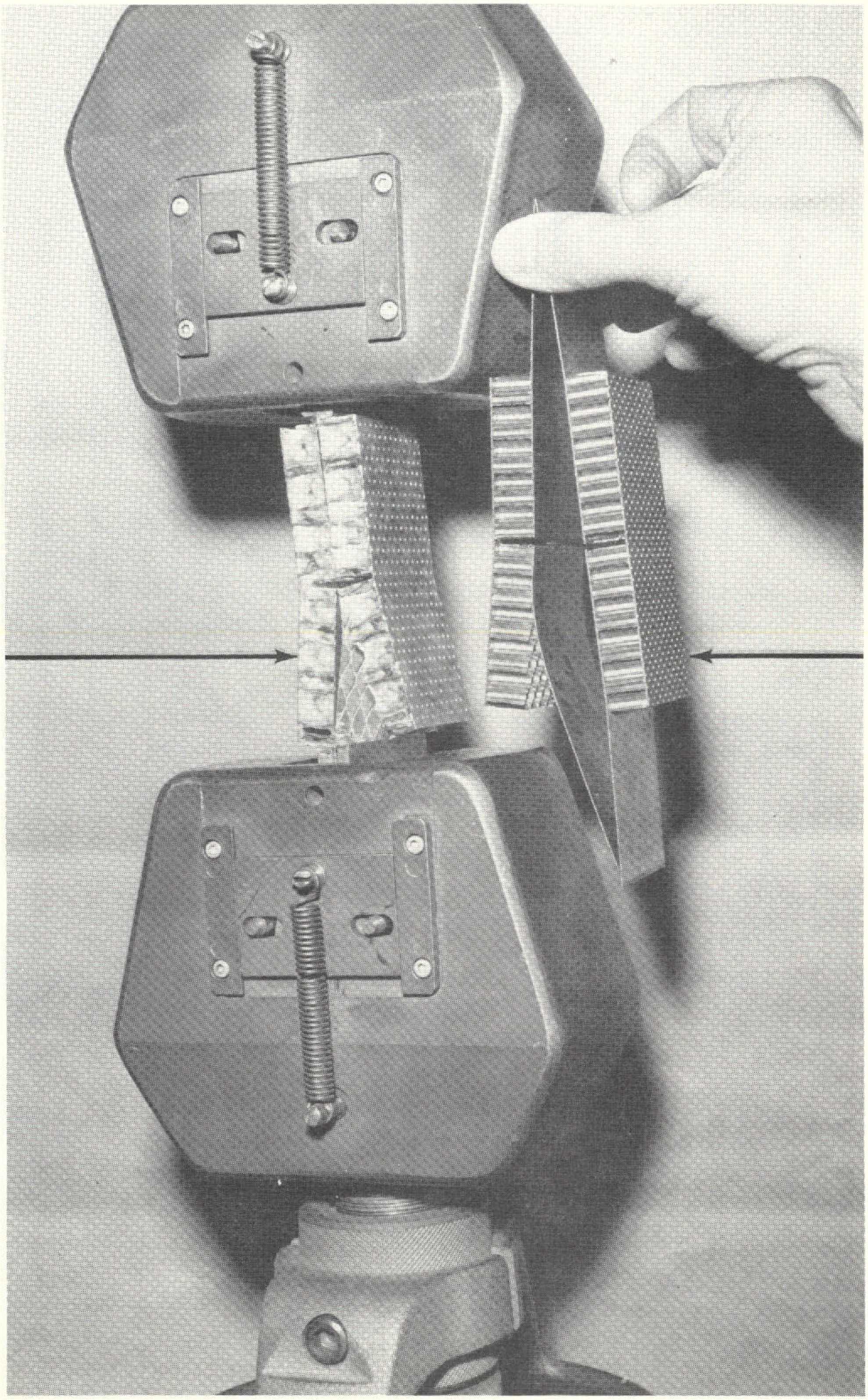

FIGURE 24. SHEAR SPECIMEN STATIC TEST FAILURES

TABLE II. SHEAR SPECIMEN FATIGUE TEST RESULTS

TEST NO.	BATCH	APPLIED LOAD P LB.	STRESS RATIO R.	NO. OF CYCLES TO FAILURE	EQUIVALENT CYCLES P = 1040 LB R = .10	FAILURE DESCRIPTION
2	B	1,000	0.10	2,000	1,700	CORE AND BOND FAILURE DUE TO LOCAL SKIN BENDING
3	C	1,600	0.10	5,000	37,000	CORE SHEAR FAILURE
4		1,200	0.10	10,000	17,500	CORE SHEAR FAILURE
6	D	1,000 1,200 1,400	0.10 TOTAL	200,000 200,000 101,000 501,000	 900,000	LOAD CHANGED LOAD CHANGED LOAD CHANGED SHEAR FAILURE OF CORE TENSILE FAILURE IN PERFORATED SKIN
7(b)	D	400	0.10	64,000		BOND FAILURE DUE TO SKIN BENDING
8(b)	D	350	0.10	41,000		BOND AND CORE FAILURE DUE TO SKIN BENDING
1 & 5 (a)	B&D	500 650 800 1,000	0.10 TOTAL	1,540,000 602,000 508,000 112,000 2,762,000	 420,000	LOAD CHANGED LOAD CHANGED LOAD CHANGED LOAD CHANGED BATCH B SPECIMEN FAILED IN BOND AND CORE SHEAR BATCH D FAILED IN PERFORATED SKIN

NOTE: (a) THESE WERE THE UNDAMAGED SPECIMENS FROM THE STATIC TEST MOUNTED BACK TO BACK TO FATIGUE TEST.
(b) SOLID SKIN NOT BACKED UP BY DOUBLER.

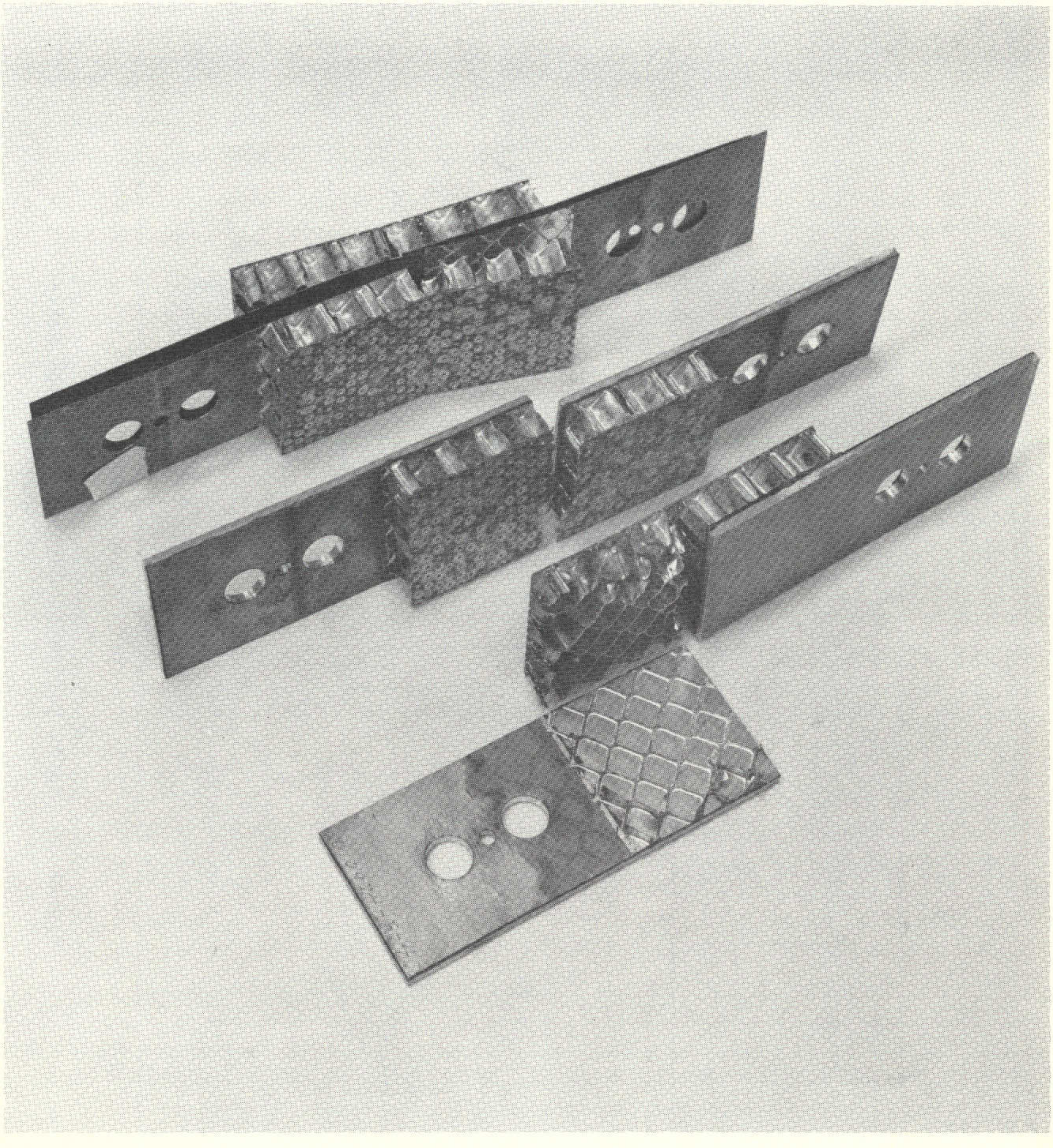

FIGURE 25. TYPICAL SHEAR COUPON FATIGUE TEST FAILURES

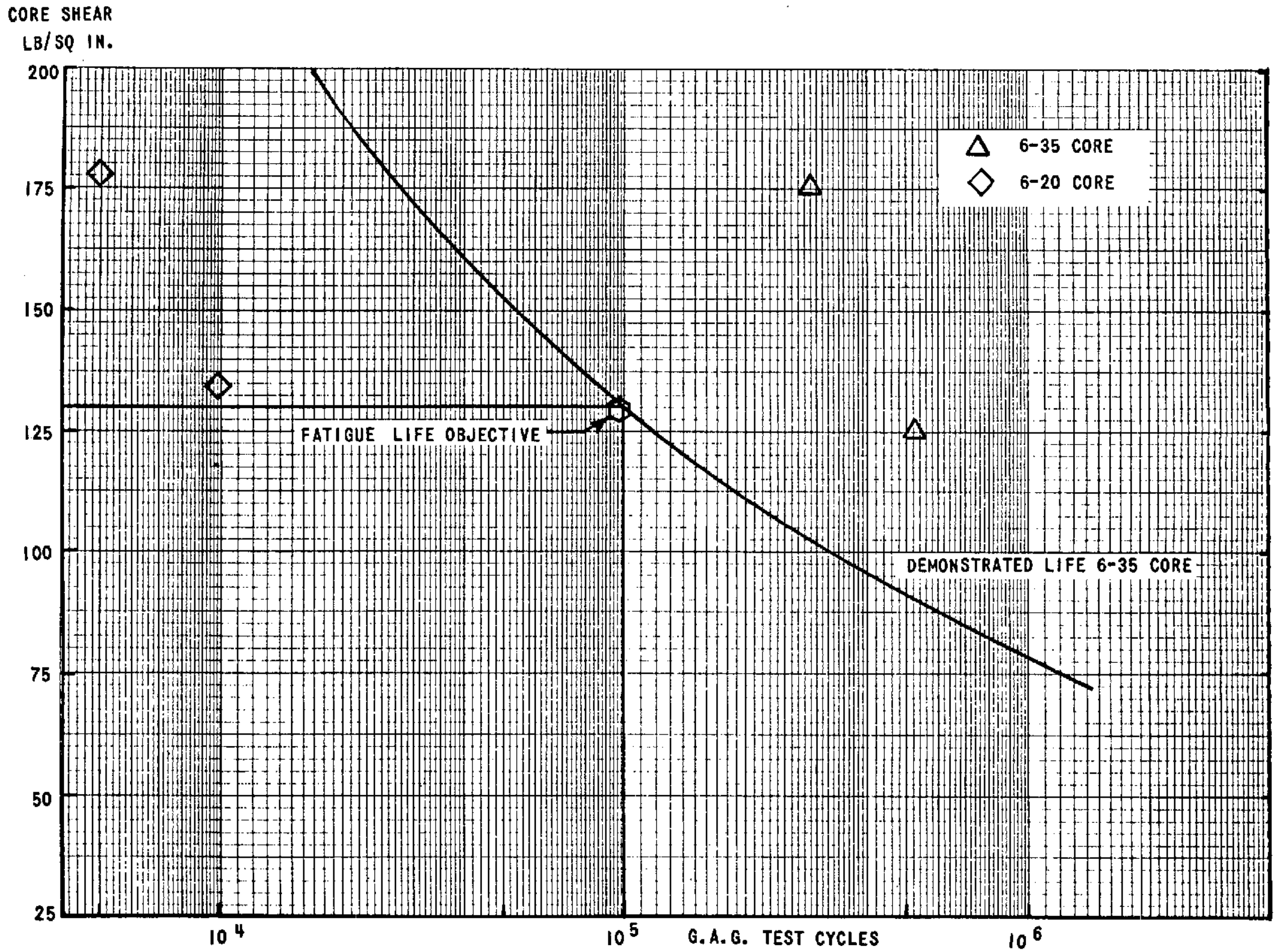

FIGURE 26. SHEAR SPECIMEN CORE SHEAR FATIGUE CURVE

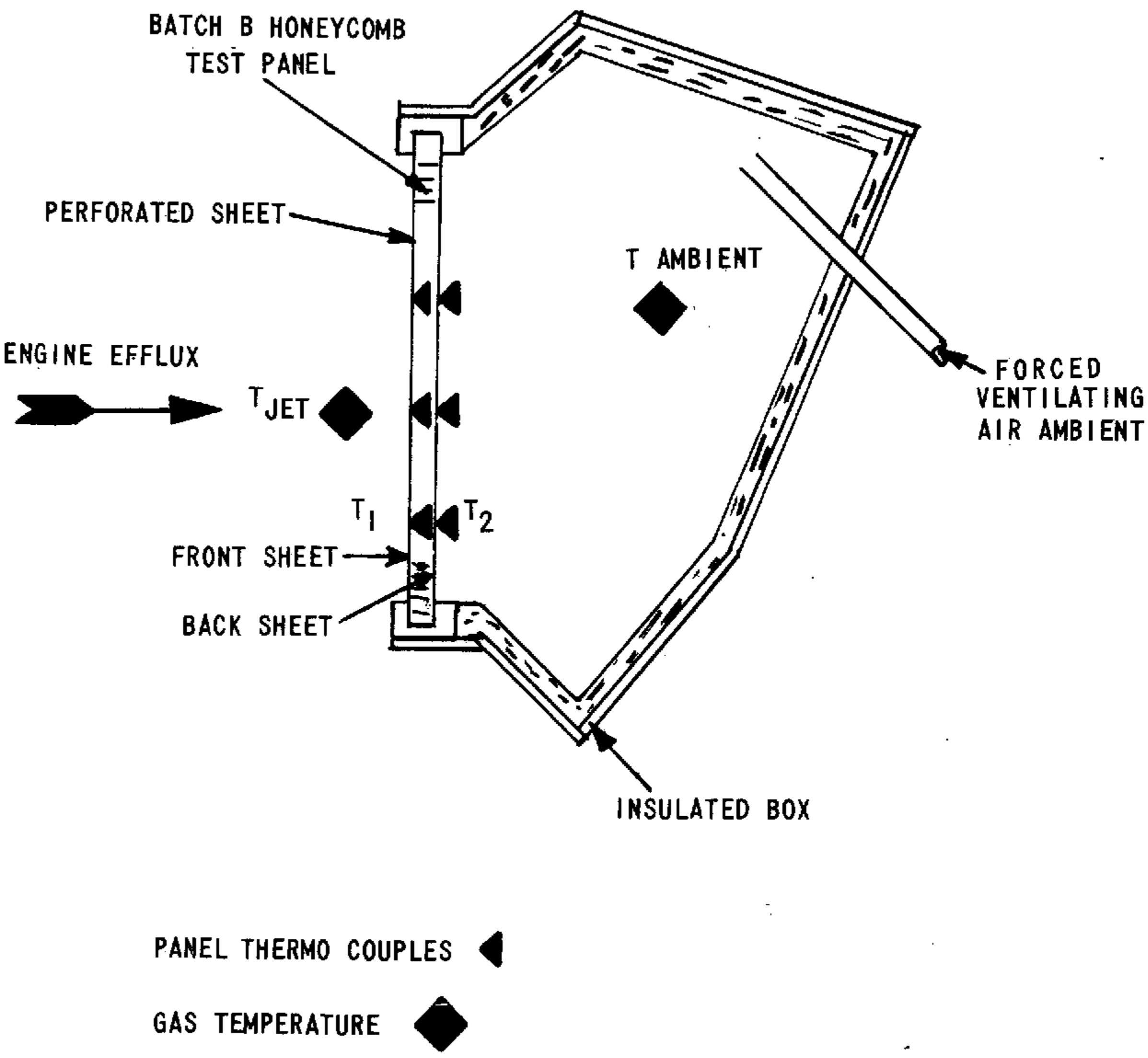

FIGURE 27. CONFIGURATION OF THERMAL TEST FIXTURE

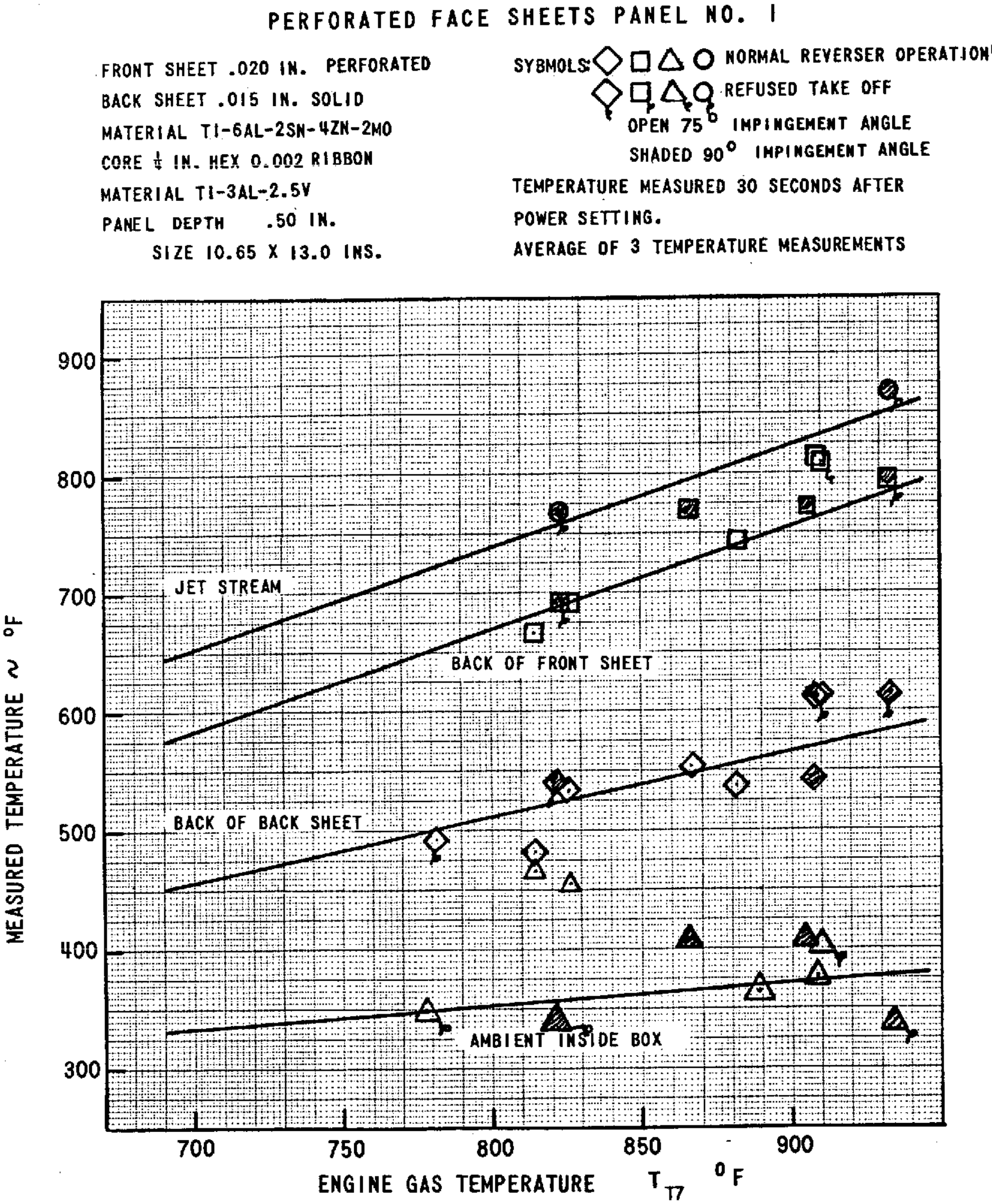

FIGURE 28. THERMAL TEST PANEL NO. I MEASURED TEMPERATURE

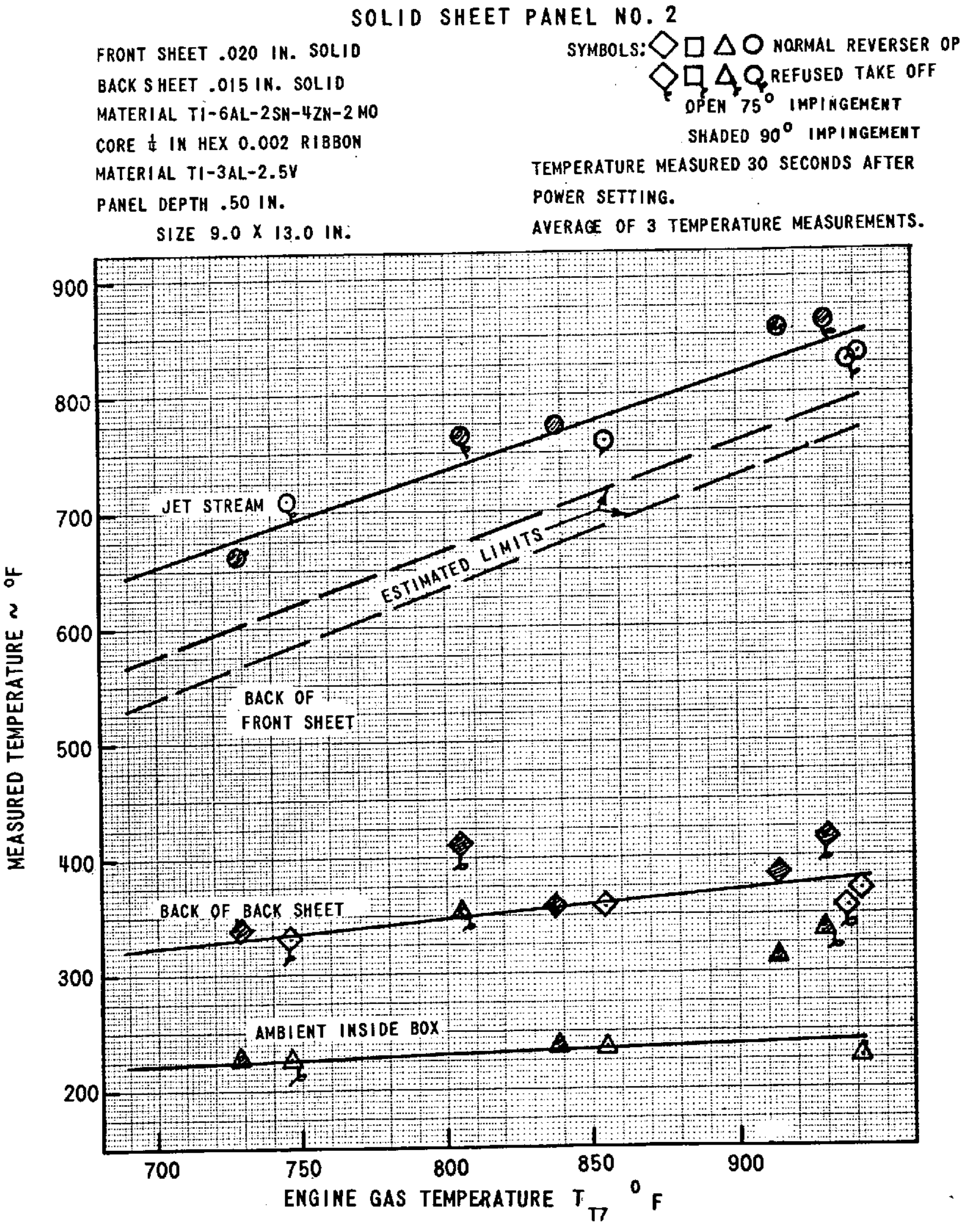

FIGURE 29 THERMAL TEST PANEL NO. 2 MEASURED TEMPERATURE

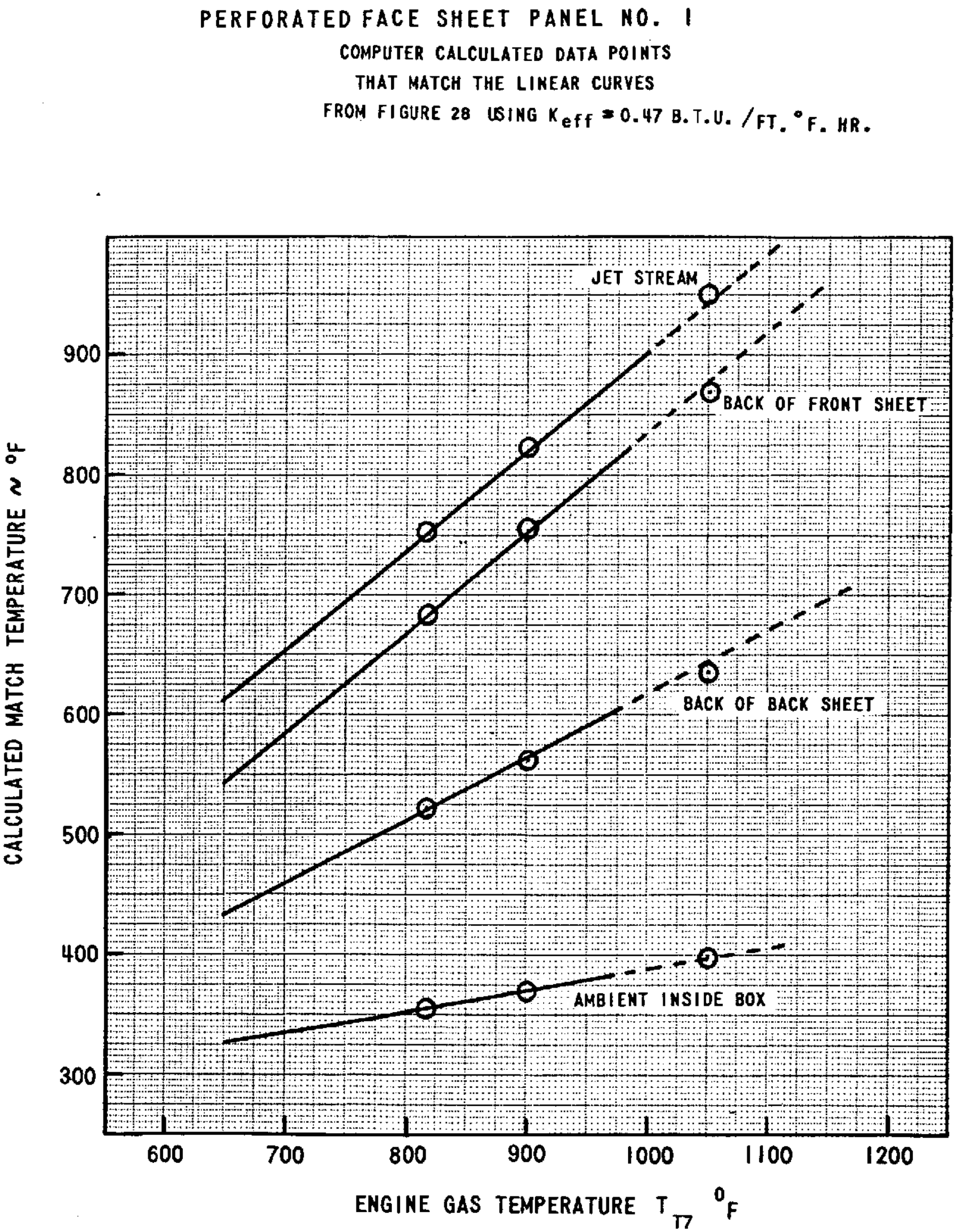

FIGURE 30 THERMAL TEST PANEL NO. I COMPUTER CALCULATED DATA POINTS

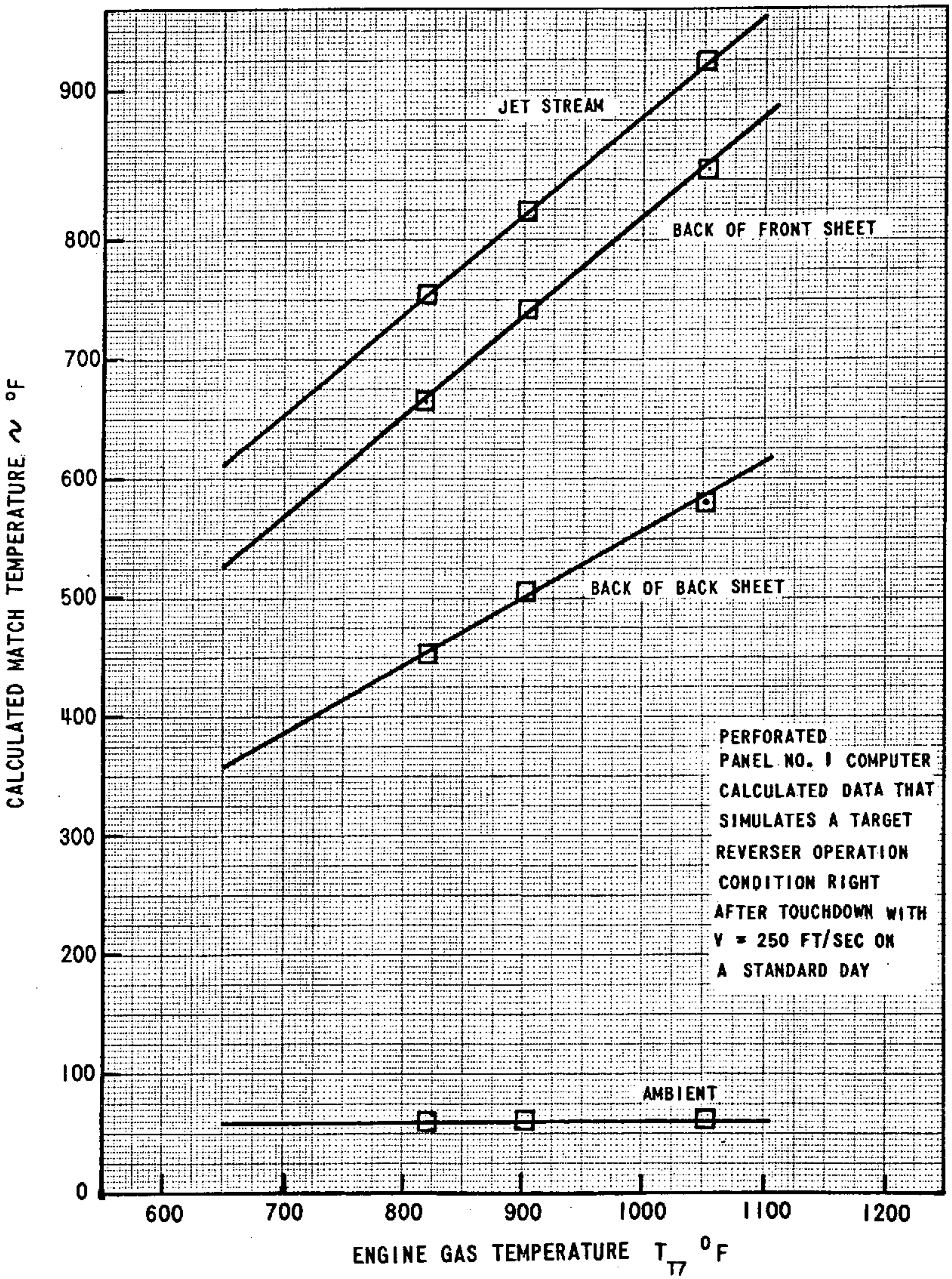

FIGURE 31 THERMAL TEST PANEL NO. 1 STANDARD DAY, NORMAL OPERATION

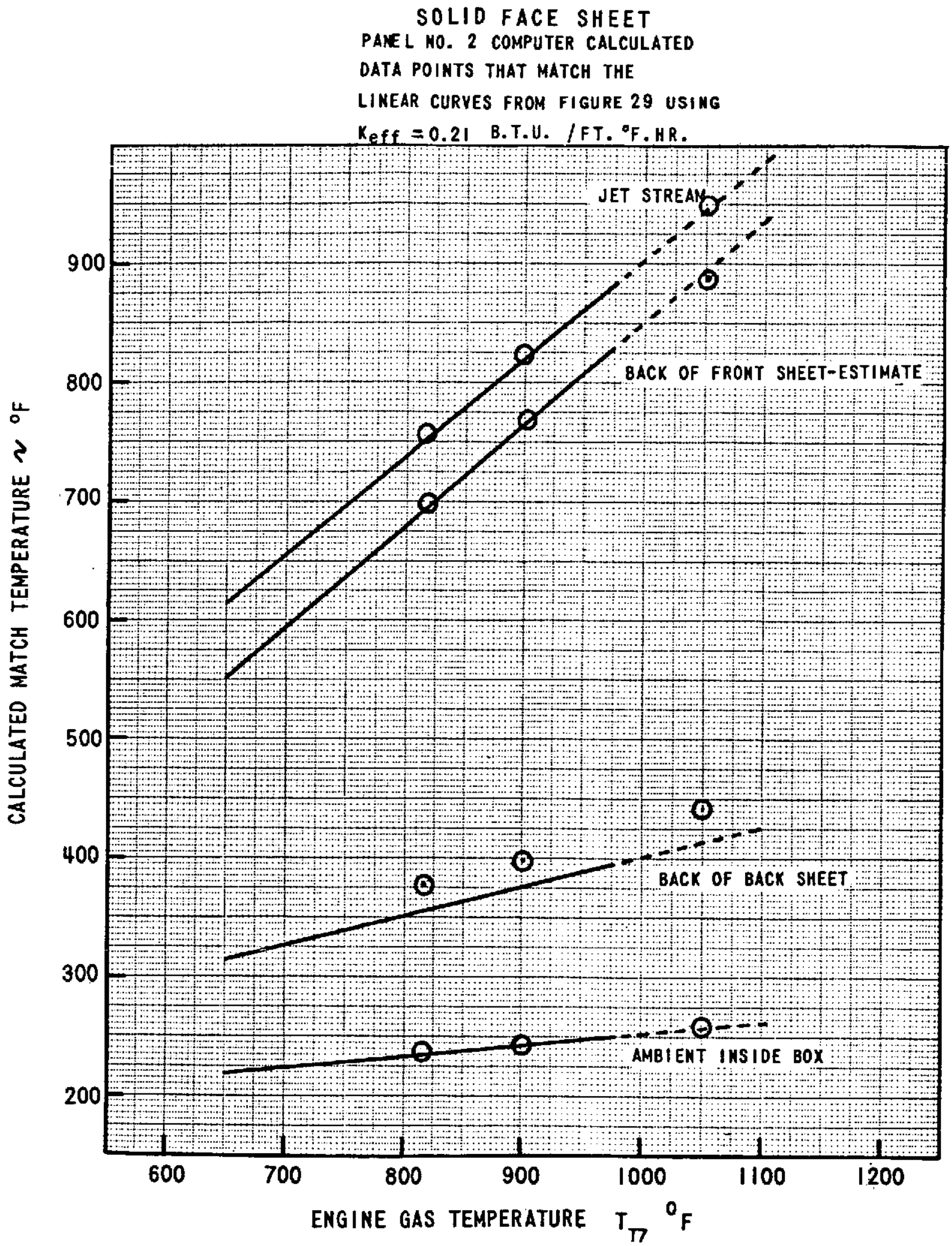

FIGURE 32. THERMAL TEST PANEL NO. 2 COMPUTER CALCULATED DATA POINTS

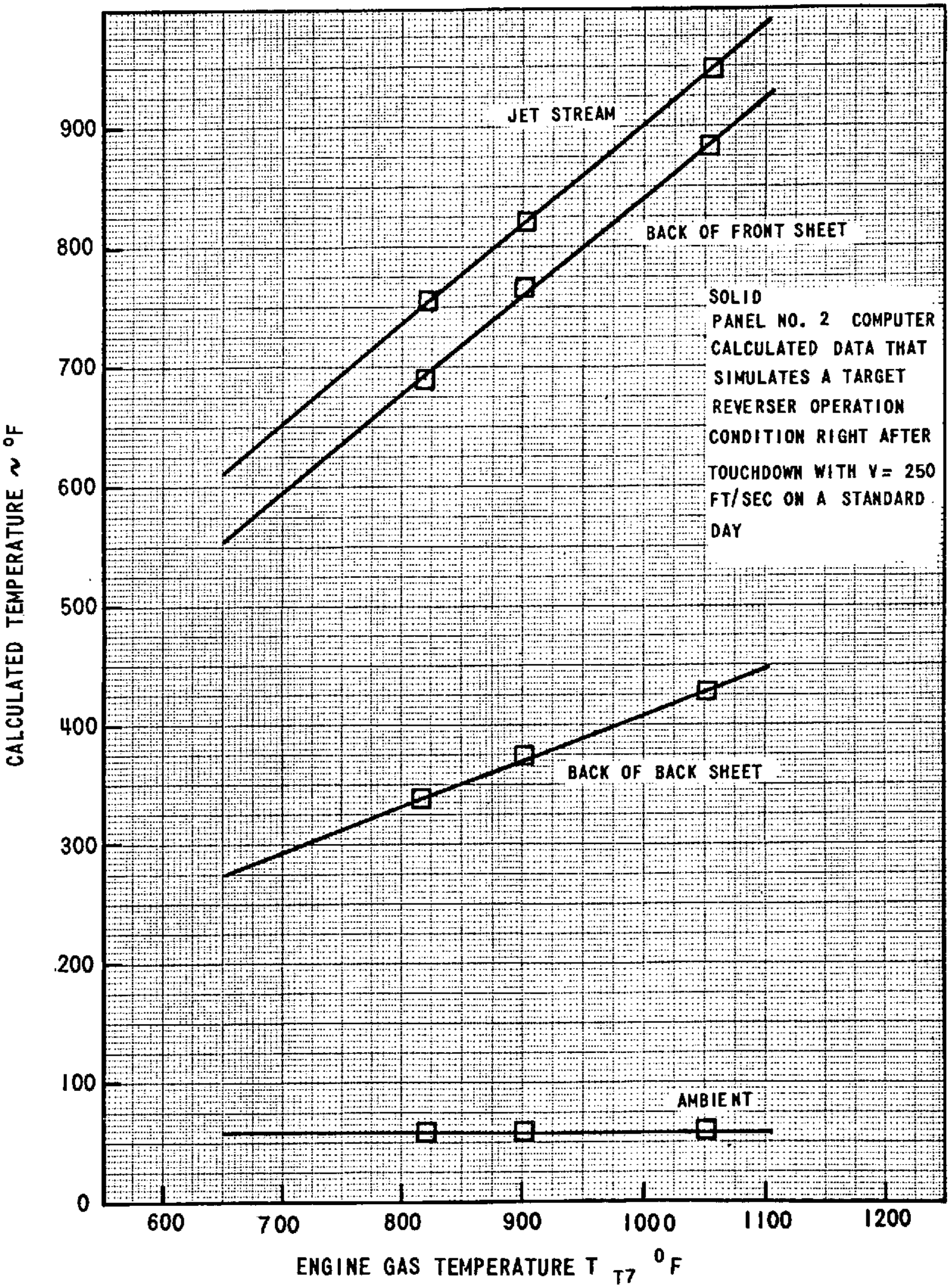

FIGURE 33. THERMAL TEST PANEL NO. 2 STANDARD DAY, NORMAL OPERATION

APPENDIX A - DATA REDUCTION

STRESS METHODS

The stress levels used for the data plots were obtained from the applied panel loads by assuming basic load distributions and using simple stress equations. Where possible, credence was given to these stress levels by comparison with the static failure stress, which is assumed to have occurred at approximately the material ultimate static stress (F_{tu}).

For titanium 6AL-4V annealed sheet

F_{tu} A value = 134,000 lb per sq in
B value = 139,000 lb per sq in

Reference 2

FLANGE PANEL

Solid skin at Chem-milled Radius.

Reference stress based on static test failure section.

Skin stress $f_t = \frac{P}{W \times t_s}$ lb/sq in

where P = Panel Load
W = Panel Width
t_s = Skin Thickness

From Table 3

Average static test failure stress

f_t = 149,000 lb/ sq in F_{tu} = 139,000 lb/sq in

PRECEDING PAGE BLANK NOT FILMED

FLANGE BENDING

Section considered at crack origins in bolt holes, Section XX.

Moment distribution in flange was assumed to be

60% at bolt

40% at flange runout

Effective flange

Width = 5d per bolt and 3 bolts per flange

Moment on Section

= .26P

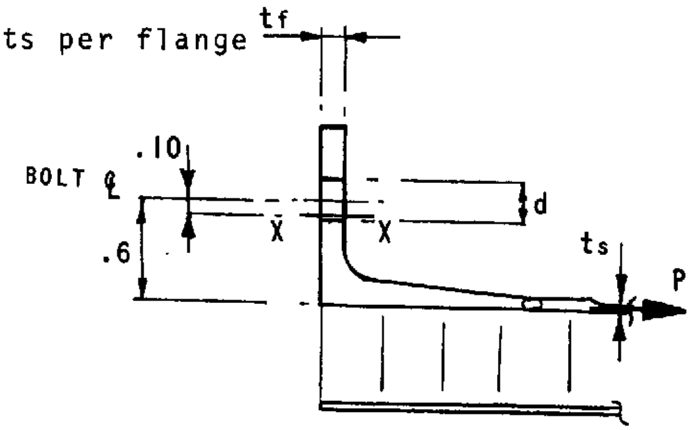

Flange bending at Section

$$\text{stress} = \frac{6 \times .26 \times P}{3 \times 5 \times d \times t_f^2} = \frac{.104\,P}{d \times t_f^2}$$

where d = bolt diameter

t_f = flange thickness

BOLT FAILURES

Bolt failures are plotted against panel load P neglecting torque preload and bolt diameter and is reduced in terms of short and long bolts.

RAIL PANEL

Solid skin at chem-milled radius.

Reference stress based on static test failure section.

Panel section constants

Area = $\cdot 25$ sq in I_{xx} = $\cdot 02$ in^4 c = $\cdot 25$ in

Panel loads due to rail load P

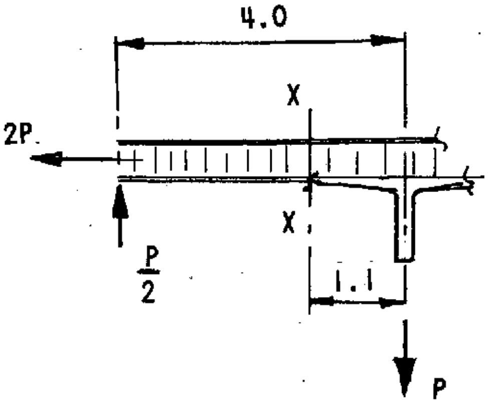

Transverse load = 2 P lb
Bending = 1.45 P lb
Stress in solid skin at Section XX.

$$f_t = \frac{2P}{\cdot 25} + \frac{1.45\ P \times \cdot 25}{\cdot 02}$$

$$= 26.13\ P$$

From Table 7

Only Test 1 failed at chem-milled radius static test failure stress

$$f_t = 26.13 \times 5250 = 137{,}200 \text{ lb/sq in}$$

$$F_{tu} = 139{,}000 \text{ lb/sq in}$$

SHEAR SPECIMEN

Shear stress is based on coupon area.

Core shear stress $f_s = \frac{P}{2 \times W \times L}$

Reference stress is based on 6-35 core 0.5 inches thick which is used in the tailpipe design.

FATIGUE DATA REDUCTION

The data reduction method used to derive from the test data the demonstrated fatigue life curves is from the proprietary BCAC Fatigue Design Manual.

This analysis is based on Weibull distribution taking into account the number of data points considered, number of test cycles achieved at each data point and the material being considered,to obtain the detail characteristic life at a selected stress level. Further modifications are made to take into account the test specimen relative size, number of details in population, and material reliability to obtain a 95% confidence and 95% reliability data point. The detail demonstrated life curve is then constructed using this point as the origin.

The life modification factors and shape of the demonstrated life curve were derived from test data and BCAC inservice fleet statistics.

THERMAL TEST DATA REDUCTION

The heat transfer through the honeycomb panel from hot engine exhaust gas to the cooling air,per unit area and ignoring radiation is given by:

$$\frac{q}{A} = \frac{\Delta T}{\frac{1}{H_I} + \frac{t_p}{K_1} + \frac{h}{K_{eff}} + \frac{t_s}{K_3} + \frac{1}{H_o}} \quad (1)$$

where q Heat flux

H_I Convection coefficient for the hot engine exhaust gas front face sheet.

H_o Convection coefficient for the cooling air, aft face sheet.

K_1 Coefficient of conductivity front face sheet

K_3 Coefficient of conductivity rear face sheet

K_{eff} Heat transfer coefficient of the honeycomb core, metal and air space.

t_p Front face sheet thickness

h Honeycomb thickness

t_s Rear face sheet thickness

ΔT Gas temperature differential front to rear of panel.

T_I Hot gas temperature

T_o Cool gas temperature

Also

$$\frac{q}{A} = \frac{\Delta T_1}{\frac{1}{H_I} + \frac{t_p}{K_1} + \frac{h}{K_{eff}} + \frac{t_s}{K_3}} \qquad (2)$$

Where $\Delta T_1 = T_I - T_4$

T_4 = Required temperature

For equal heat transfer rate Equation 1 = Equation 2.

Hence required temperature can be determined in terms of known parameters.

Solution of these equations was programmed for the 6600 computer and was used to iterate on K_{eff} using representative coefficients K_1, K_2, H_I and H_o until the measured specimen temperatures were obtained.

The values of K_{eff}, H_o, H_I used to match the test results were then kept constant and the panel temperatures under different operating conditions and temperatures were determined.

REFERENCES

General Reference

1. Aluminum brazed titanium: Report No. FAA-SS-73-5 Vols. 1 through 8, SST Technology Follow-On Program Phase II Development and Evaluation of the Aluminum-Brazed Titanium System. By S. D. Elrod, D. T. Lovell, May 1974.

   a. Report No. FAA-SS-73-5-4 Table 2.5, Page 27

   b. Report No. FAA-SS-73-5-5 Chapter 6.4, Page 139

   c. Report No. FAA-SS-73-5-8

2. Military Standardization Handbook Metallic Materials and Elements for Aerospace Vehicle Structures. MIL-HDBK-5B, Sept. 1971, Chapter 5.

REPORT DISTRIBUTION LIST

Addressee		No. of Copies
1. NASA Lewis Research Center 21000 Brookpark Road Cleveland, OH 44135		
Attention: Report Control Office	MS: 5-5	1
Library	MS: 60-3	2
R. W. Schroeder	MS: 501-5	1
G. K. Sievers	MS: 501-7	23
F. O. Driscoll	MS: 500-206	1
N. T. Musial	MS: 500-113	1
M. A. Beheim	MS: 86-1	1
D. N. Bowditch	MS: 86-1	1
F. J. Barina	MS: 500-211	1
D. C. Mikkelson	MS: 86-1	1
2. NASA Scientific and Technical Information Facility Attention: Acquisitions Branch P. O. Box 33 College Park, MD 20740		10
3. NASA Headquarters 600 Independence Avenue, S. W. Washington, DC 20546		
Attention: Code RJ/William H. Roudebush		6
Code RL/Harry W. Johnson		1
Code RO/Kenneth E. Hodge		1
4. Environmental Protection Agency Crystal Mall, Bldg. 2 1921 Jefferson Davis Highway Arlington, VA 22202		
Attention: John Schettino	MS: AW-571	1
William Sperry	MS: AW-571	1
5. Federal Aviation Administration 800 Independence Avenue, S. W. Washington, DC 20591		
Attention: Robert J. Koenig (Code ARD-551)		1
James F. Woodall (Code ARD-500)		1
6. Office of Environmental Quality 800 Independence Avenue, S. W. Washington, DC 20591		
Attention: John O. Powers (Code AEQ-2)		1
Richard P. Skully (Code AEQ-1)		1

Addressee			No. of Copies
7. Department of Transportation 400 7th Street, S. W. Washington, DC 20590			
Attention:	Charles R. Foster		1
	Bernard Maggin (Code TST-51)		1
8. NASA Langley Research Center Hampton, VA 23365			
Attention:	Harry T. Norton, Jr.	MS: 249A	1
	Thomas F. Bonner, Jr.	MS: 257	1
9. NASA Ames Research Center Moffett Field, CA 94035			
Attention:	Stuart Treon	MS: 227-5	1
	Jim Monford	MS: 227-5	1
10. NASA Flight Research Center P. O. Box 273 Edwards, CA 93523			
Attention:	Donald Bellman	Room 2106	1
11. United Air Lines SFO EG San Francisco International Airport San Francisco, CA 94128			
Attention:	L. C. Ellis		1
	R. A. Gustafson		1
12. General Electric Company Acoustic Design Technology Cincinnati, Ohio 45215			
Attention:	Robert Lee		1
13. McDonnell Douglas Corporation 3855 Lakewood Boulevard Long Beach, CA 90846			
Attention:	W. A. Alden		1
	J. N. Thomas		1
	J. E. Donelson		2
14. Pratt & Whitney Aircraft 400 Main Street East Hartford, CT 06108			
Attention:	G. M. McRae		2
15. Rohr Corporation P. O. Box 878 Chula Vista, CA 92012			
Attention:	Steve Beggs		1

Addressee	No. of Copies
16. General Electric Company Aircraft Engine Group - E198 Cincinnati, OH 45215 Attention: John T. Kutney	1